American Mineralogist, Volume 66, pages 1107–1134, 1981

Hydrous pyriboles and sheet silicates in pyroxenes and uralites: intergrowth microstructures and reaction mechanisms

DAVID R. VEBLEN[1] AND PETER R. BUSECK

Departments of Geology and Chemistry
Arizona State University, Tempe, Arizona 85281

Abstract

A wide variety of intergrowth microstructures have been observed with high-resolution transmission electron microscopy in eight different pyroxene specimens that have been partially or wholly altered to other minerals. The product phases of the alteration reactions include amphibole, clinojimthompsonite, chain-width disordered pyribole, and several sheet silicates. Textural considerations indicate that there are a number of different paths for pyroxene hydration reactions. These include the simple paths pyroxene → amphibole, pyroxene → clinojimthompsonite, and pyroxene → sheet silicate, as well as more complicated, stepwise paths, such as pyroxene → amphibole → sheet silicate and pyroxene → clinojimthompsonite → sheet silicate. In some cases, multiple reaction paths are observed in the same specimen. The microstructures indicate that in addition to multiple paths for reaction, there may be multiple mechanisms by which a specific reaction may occur. For example, replacement of pyroxene by amphibole or other hydrous pyriboles can take place either by the nucleation and growth of narrow lamellae of the product mineral, or by a bulk replacement mechanism along a broad reaction front. Replacement of pyroxene by amphibole takes place in such a way that multiple nucleation events may result in several different types of out-of-phase boundaries in the product amphibole.

The distinction between exsolution and alteration reaction as a mechanism for the formation of narrow amphibole lamellae in pyroxenes is chemical, rather than structural. The determination of which mechanism has operated must therefore be based on chemical and textural arguments. It is concluded that all cases of pyroxene replacement by amphibole that have been reported are at least consistent with an alteration mechanism, while the textures occurring in some specimens are clearly inconsistent with an exsolution mechanism. With presently available data it is not possible to identify the physical and chemical conditions that lead to specific types of reaction behavior.

Failure to recognize the presence of finely intergrown hydrous pyriboles in pyroxene could lead to significant errors in the application of geochemical techniques relying on cation partitioning, such as geothermometric and geobarometric methods utilizing pyroxene chemistry.

Introduction

During the past few years, there have been numerous reports of amphibole lamellae intergrown with pyroxenes of a wide range of compositions and occurring in a variety of geological environments. For example, pyroxene–amphibole intergrowths occur in augites from basic intrusions, such as the Skaergaard, the Bushveld, and the Palisades Sill; in omphacites from eclogites; in jadeites from glaucophane schists; and in augites, orthopyroxenes, and diopsides from peridodites, lherzolites, harzburgites, and gabbros (Smith, 1977; Papike *et al.*, 1969; Yamaguchi *et al.*, 1978; Desnoyers, 1975; Bown and Gay, 1959; Francis, 1976; Nakajima and Ribbe, 1980; Isaacs *et al.*, 1980). In addition, intergrowths of pyroxene with sheet silicates and triple-chain silicates have recently been reported (Veblen and Buseck, 1977, 1980; Buseck and Veblen, 1978). Clearly, pyroxenes can intergrow with the entire range of hydrous biopyriboles, from amphiboles to

[1] Present address: Department of Earth and Planetary Sciences, The John Hopkins University, Baltimore, Maryland 21218.

0003–004X/81/1112–1107$02.00

micas and talc. Such intergrowths are frequently on a scale finer than the resolution of a petrographic microscope. Even when petrographically invisible, however, hydrous biopyriboles could have significant effects on cation partitioning behavior, and hence on the use of pyroxenes for geothermometry, geobarometry, and trace element partitioning studies. Hydrous biopyriboles intergrown with pyroxenes are therefore of petrological as well as mineralogical importance.

The structural basis for the intergrowth of pyroxenes and amphiboles has been discussed by Thompson (1970, 1978), Chisholm (1973, 1975), and Yamaguchi *et al.* (1978). Most of the crystal-chemical concepts that are applicable to hydrous biopyribole intergrowths are also applicable to intergrowths that include pyroxene. As a result, the present paper draws heavily on our previous work with intergrowths produced by hydration of amphibole (Veblen *et al.*, 1977; Veblen and Burnham, 1978a,b; Veblen and Buseck, 1979a,b,c; 1980). Not surprisingly, hydration mechanisms in pyroxenes are often exactly analogous to homogeneous replacement mechanisms in amphiboles, but the present study also suggests mechanisms in some pyroxenes that were unanticipated from the earlier work on amphiboles.

It is our aim in this paper to describe the microstructures produced by alteration reactions in eight different specimens, as seen with high-resolution transmission electron microscopy (HRTEM). Because most of the features reported here have not been described previously, and because many of them have important genetic implications, the descriptions of the specimens are intentionally quite detailed. Concentrating on several specimens makes it abundantly apparent that there is remarkable diversity in the reaction behavior exhibited by altering pyroxenes. We have chosen to divide the specimens into two broad categories: (1) pyroxenes that contain lamellae of hydrous pyriboles and (2) pyroxenes that have been largely or completely replaced by other phases.

Perhaps the most important conclusion of this work is that there are a number of different distinguishable mechanisms of hydration reaction that can operate in different specimens, or, in some cases, even in a single pyroxene crystal. In connection with these reaction mechanisms, we also address the question of whether amphibole lamellae in pyroxenes are the products of exsolution or hydration during alteration (Papike *et al.*, 1969; Smith, 1977; Yamaguchi *et al.*, 1978); although the problem cannot be rigorously resolved, we believe that all of our observations and those that have been reported in the literature are consistent with an alteration origin. Finally, because the cation partitioning behavior of pyroxenes containing even small amounts of hydrous biopyribole may be quite anomalous, we evaluate the effects of using unrecognized pyroxene–amphibole intergrowths for simple clinopyroxene–orthopyroxene geothermometry.

Experimental techniques, image interpretation, and specimen chemistry

Electron microscopy was performed as described by Veblen and Buseck (1979a). All specimens were ion thinned, usually from petrographic thin sections having the pyribole *c*-axis normal to the plane of the section; the thin foils were then carbon coated. The specimens used in this study are listed in Table 1. Interpretation of the HRTEM images is analogous to

Table 1. Sources of specimens used in this study

Specimen	Locality	Source	Specimen Number
Harzburg orthopyroxene	Harzburg, Germany	Manchester University (Smith, 1977)	13804
Palisades sill augite	Englewood Cliffs, New Jersey	D. Veblen	EC39
Salt Lake Crater augite	Salt Lake Crater, Hawaii	A. Boettcher	69-SAL-37
Roberts Victor Al-clinopyroxene	Roberts Victor Mine, South Africa	J. Smyth (Smyth & Hatton, 1977)	SRV-1
Loch Raven tremolite after diopside	Loch Raven, Baltimore, Maryland	U. S. National Museum	136525
White Picacho spodumene	White Picacho pegmatite district, Arizona	D. London (London, 1979)	MNO205
Copper Mountain uralite	Copper Mountain, Prince of Wales Island, Alaska	U. S. National Museum	R7780-3
Romanian uralite	Juliana Quarry, Ocna de Fier, Romania	D. Burt	7-26-73

that presented by Veblen and Buseck (1979a, 1980), which has been confirmed by dynamical diffraction and imaging calculations.

Analytical data on the Roberts Victor Al-clinopyroxene and the Romanian uralite have been reported by Smyth (1980) and Veblen and Buseck (1979b), respectively. London (1979) discusses the chemistry of the White Picacho spodumene breakdown reactions, but the spodumene itself was not analyzed because of high lithium content. Electron microprobe analyses of the remaining specimens used in this study are presented in Table 2. Analyses were performed with a Tracor Northern TN2000 energy-dispersive X-ray analyzer on a Cameca MS46 microprobe. Each of the analyses in Table 2 represents the average of twenty point analyses, with the exception of the Salt Lake Crater analyses, which are averages of ten points. The charge balance criteria at the bottom of the table indicate the number of unbalanced charges per formula unit, assuming all iron to be Fe^{2+}. In all cases, the charge can be balanced perfectly by allowing very small amounts of Fe^{3+}.

Table 2 shows that the Harzburg orthopyroxene is a bronzite and the Palisades Sill specimen is a magnesian augite. The amphibole analyses from the Salt Lake Crater specimen were performed on rods and blebs of amphibole included in the pyroxene; the pyroxene is an aluminous augite, and the amphibole is a kaersutite. The Loch Raven specimen is a very pure tremolite. The amphibole of the Copper Mountain uralite, an actinolite, was very inhomo-

Table 2. Electron microprobe analyses of some of the specimens used in this study

Specimen	Harzburg Orthopyroxene	Palisades Sill Augite	Salt Lake Crater Pyroxene	Intergrowth Amphibole	Loch Raven Tremolite	Copper Mountain Uralite
Na_2O		0.3	0.7	2.8		0.4
MgO	31.2	14.9	11.3	11.2	24.7	15.1
Al_2O_3	2.2	1.9	9.0	15.1		1.8
SiO_2	55.6	52.1	46.9	39.5	59.5	53.7
K_2O				0.7		0.1
CaO	2.1	18.0	21.4	11.3	13.7	12.5
TiO_2	0.1	0.5	2.1	4.9		
Cr_2O_3	0.6					
MnO	0.2	0.3	0.1	0.1		0.4
FeO*	8.5	12.1	8.5	12.4	0.2	14.1
Total	100.4	100.1	100.0	98.0	98.1	98.1
			Structural Formulae			
Number of oxygens	6	6	6	23	23	23
Tetrahedral:						
Si	1.94	1.95	1.75	5.84	8.02	7.77
Al	0.06	0.05	0.25	2.16		0.23
Total	2.00	2.00	2.00	8.00	8.02	8.00
Octahedral:						
Mg	1.62	0.83	0.63	2.46	4.96	3.25
Al	0.03	0.03	0.15	0.48		0.08
Ca	0.08	0.72	0.86	1.79	1.98	1.94
Ti		0.02	0.06	0.55		
Cr	0.02					
Mn	0.01	0.01		0.01		0.04
Fe*	0.25	0.38	0.27	1.53	0.02	1.70
Na		0.02	0.05	0.18		
Total	2.01	2.01	2.02	7.00	6.96	7.01
A-site						
Na				0.63		0.11
K				0.13		0.01
Total				0.76		0.12
Charge Balance	$Al^{O}+Cr+2Ti-Al^{T}=$ -0.01	$Al^{O}+2Ti-Na-Al^{T}=$ 0.00	$Al^{O}+2Ti-Na-Al^{T}=$ -0.03	$Al^{O}+2Ti+Na^{A}+K$ $-Na^{O}-Al^{T}=$ 0.00		$Al^{O}+Na^{A}+K-Al^{T}+$ -0.03

* All iron calculated as Fe^{2+}.
** Superscripts O and T refer to octahedral and tetrahedral, respectively.

geneous, exhibiting Al contents ranging from 0.7% to 3.4%, for example. Such inhomogeneity is presumably the result of formation by alteration at relatively low temperatures.

Pyroxenes containing lamellae of hydrous pyriboles

Harzburg orthopyroxene

This orthopyroxene is from a harzburgite that is slightly altered but has no amphibole visible in petrographic thin section. It is from the same specimen as that used by Smith (1977), who observed amphibole lamellae in the clinopyroxene using conventional TEM techniques. The orthopyroxene crystal that was examined with HRTEM was surrounded by talc and serpentine. A *c*-axis electron diffraction pattern from the interior of the crystal (Fig. 1a) shows both pyroxene and amphibole diffractions. The amphibole diffractions are heavily streaked in the b^* direction, consistent with very narrow (010) lamellae of amphibole embedded in pyroxene. A diffraction pattern from near the edge of the crystal (Fig. 1b) shows only very weak pyroxene diffractions and is characteristic of amphibole with extensive chain-width disorder.

High-resolution imaging shows that the interior of the orthopyroxene grain contains very narrow amphibole lamellae parallel to (010) (Fig. 2a). These lamellae make up about 10% of the specimen, by volume. Lamellae that are 2, 4, 6, 8, or 10 amphibole chains wide are the most common. Of the nearly 1,000 lamellae that were observed, only two had widths corresponding to an odd number of amphibole chains. The most likely explanation for the even lamellar widths is that the lamellae formed by reaction (either hydration or exsolution) from primary pyroxene. In growing into the pyroxene, the lamellae rigorously obeyed the second rule for coherent replacement in biopyriboles set forth by Veblen and Buseck (1980): if the number of silicate chains in a growing lamella is even, the lamella must replace an even number of chains in the host material; if the lamella has an odd number of chains, it must replace an odd number in the host. Violation of this rule results in either the creation of planar defects or severe structural distortion at the termination of the lamella. In the present case, a lamella that is two amphibole chains wide (even) can coherently replace a slab of pyroxene structure four chains wide (also even). If a lamella of amphibole only one chain wide (odd) were to replace a slab of pyroxene two chains wide (even), an energetically unfavorable planar fault or distortion would occur. The same is true for any other lamellar width containing an odd number of amphibole chains. The fact that the lamellae in this specimen contain even numbers of amphibole chains, almost without fail, is a striking testament to the strong structural control exercised by the reaction mechanism.

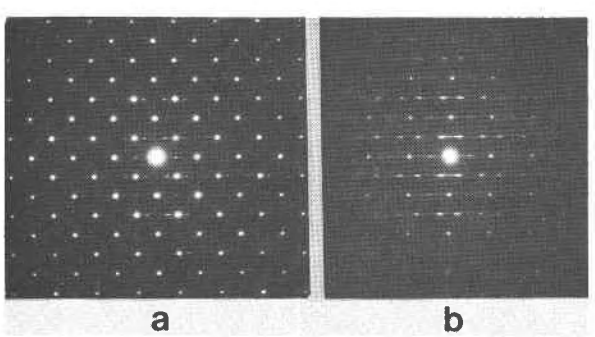

Fig. 1. Harzburg orthopyroxene. (a) A *c*-axis electron diffraction pattern from the interior of an orthopyroxene crystal. Sharp pyroxene diffractions and streaked amphibole diffractions are present. a^* is vertical and b^* is horizontal. (b) Diffraction pattern from the edge of the same crystal. The pattern is characteristic of amphibole with extreme chain-width disorder.

Terminations of amphibole lamellae two chains wide have been observed (Fig. 2b). Following nucleation, a lamella presumably grows through the crystal by consuming pyroxene; the mechanism would be analogous to that discussed by Veblen and Buseck (1980) for the growth of wide-chain zippers in amphibole, with much of the necessary diffusion between the crystal and its surroundings taking place along tunnels at the terminations of the lamellae. Widening of a lamella can take place by the nucleation and growth of ledges two amphibole chains wide (Fig. 2c). It is also possible that these lamellae could grow by more than two chains at a time (with a ledge four amphibole chains wide, for example), but no experimental evidence for this has been found.

One of the two lamellae observed to contain an odd number of amphibole chains is shown in Figure 2d. This lamella, which is 27 amphibole chains wide, is the widest lamella (about 245A wide) observed in this orthopyroxene. The lamella also has other unique features: the opposing ledges on either side of the lamella are only one amphibole chain wide. Strain contrast in the neighborhood of the ledges indicates that there is structural distortion accompanying these defects.

High-resolution imaging of the material near the

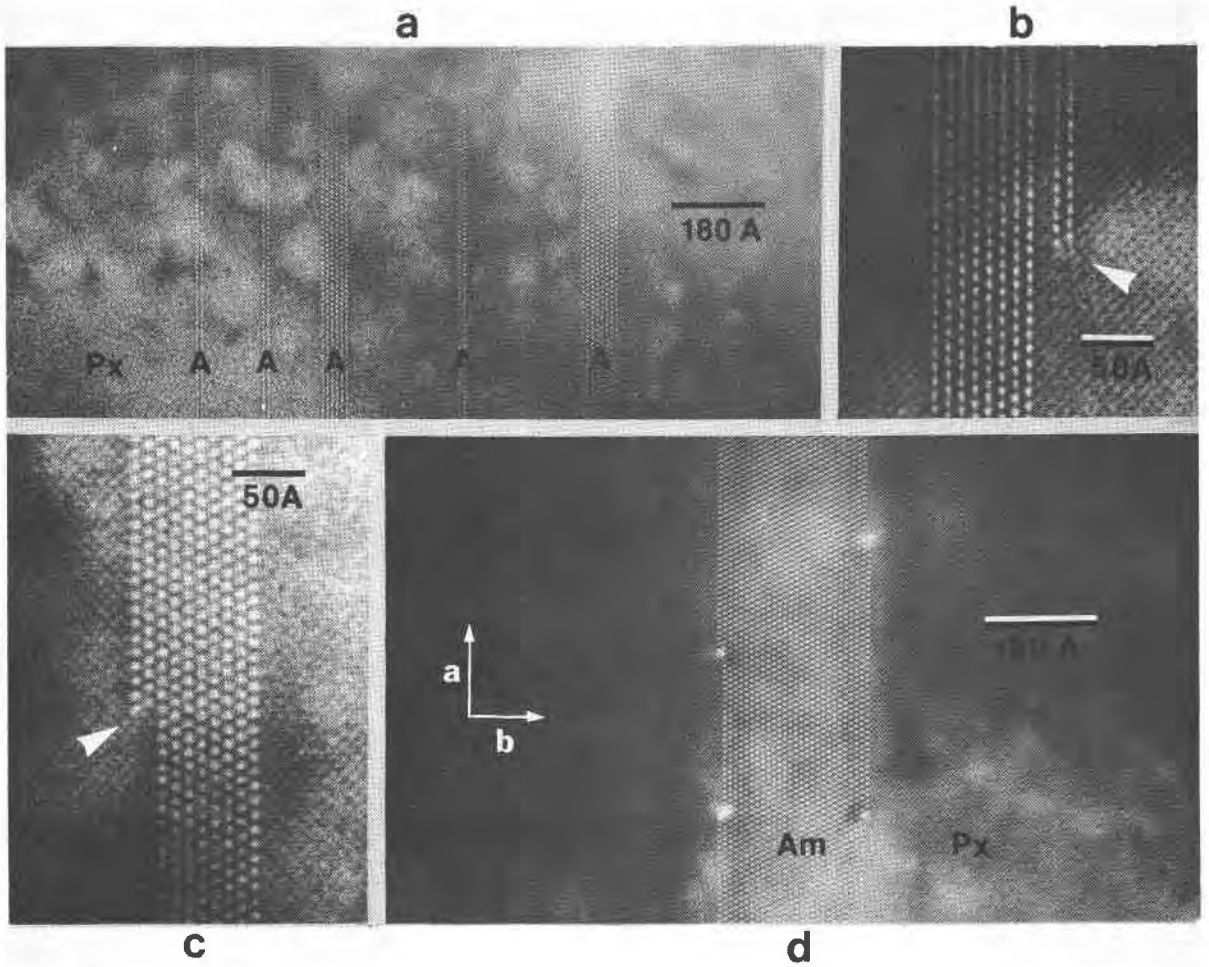

Fig. 2. Harzburg orthopyroxene. (a) Amphibole lamellae ("A") oriented parallel to (010) in the pyroxene matrix. From left to right, the widths of the lamellae are 2, 2, 6, 2, and 8 amphibole chains. (b) The termination (arrowed) of an amphibole lamella two chains wide. (c) A ledge two chains wide on an amphibole lamella. (d) The widest amphibole lamella (27 chains wide) observed in this specimen. This is one of only two lamellae observed to have an odd width. Strain contrast accompanies ledges that are one amphibole chain wide, which can be seen most easily by viewing the figure at a low angle parallel to the interfaces.

boundaries of the pyroxene crystal shows it to consist of pyribole with single, double, triple, and wider chains, intergrown with talc (Fig. 3). It is not known whether this disordered mixed biopyribole grew simultaneously with the amphibole lamellae in the interior of the crystal, or if it was formed at a later stage of alteration, following amphibole growth.

Palisades Sill augite

This augite specimen is from a diabase near the center of the Palisades Sill (about 200 meters from the lower contact). The crystals studied show no indications of alteration when examined with a petrographic microscope. HRTEM study confirms that the specimen consists almost entirely of healthy pyroxene: augite predominates, with (001) pigeonite lamellae and (100) lamellae of orthopyroxene, some of which display extreme stacking disorder. Along fractures, however, local hydration has occurred, resulting in a variety of reaction microstructures.

Much of the alteration appears to have proceeded by the growth of (010) triple-chain lamellae ("zippers") into the pyroxene. Figure 4a shows the terminations of several of these zippers. The growth of triple-chain material, rather than amphibole, is consistent with the replacement rules of Veblen and Buseck (1980); a zipper of double-chain material

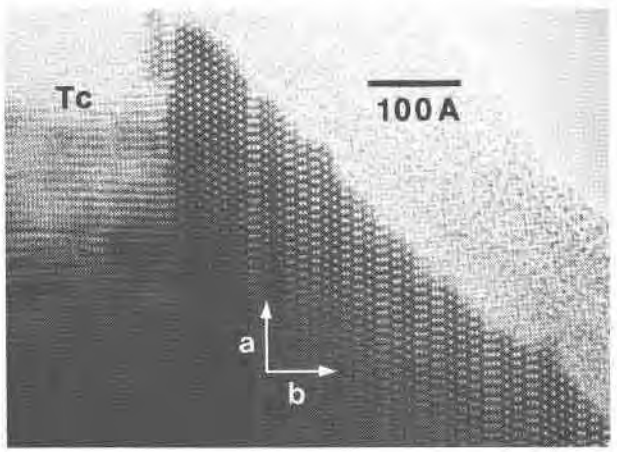

Fig. 3. Harzburg orthopyroxene. Mixed-chain silicate containing single, double, triple, and wider chains, intergrown with talc. The broad, mottled band in the upper right is amorphous material adjacent to the edge of the specimen.

one chain wide cannot coherently replace pyroxene, whereas a triple-chain zipper can. The factors that determine whether the reaction product will be triple-chain zippers or amphibole lamellae of even width are unknown, however. In some areas of pyroxene, numerous doubly-terminated triple-chain zippers occur (Fig. 4b), representing pervasive nucleation of wide-chain material. Patches of talc are also common in such regions.

Typically, a zone of invading triple-chain lamellae lies between unaltered pyroxene and sheet silicate (talc or mixed talc and serpentine). The triple-chain material thus appears to be an intermediate product in the reaction sequence pyroxene → triple-chain silicate → talc. In other places, as shown in Figure 5a, ordered triple-chain silicate, disordered wide-chain silicate, and talc all appear to be consuming pyroxene directly. In Figure 5b, talc appears to have directly replaced orthopyroxene along a fracture.

In addition to wide-chain and sheet silicates, there is also amphibole present in this Palisades augite. In some places, the amphibole occurs along fractures with triple-chain material in contact with pyroxene (Fig. 6a,b), while in other areas, blebs or rods of perfectly ordered amphibole up to several tenths of a micron in diameter occur in the augite. These blebs are not obviously associated with fractures. The contact between an amphibole bleb and pyroxene is shown in Figure 6c. These blebs could have grown by the direct consumption of pyroxene, or they may represent early lamellae of amphibole that formed by alteration or exsolution and later adjusted their boundaries into a lower-energy configuration. In still other areas, the amphibole contains numerous terminating zippers of wide-chain silicate, along with displacive planar faults associated with some of the terminations (Fig. 7). Features

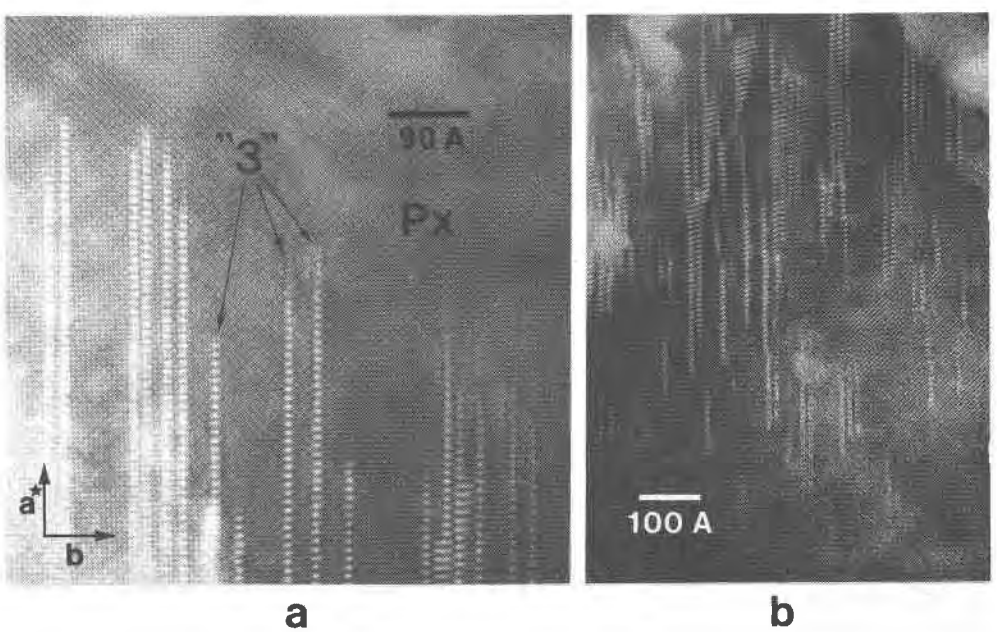

Fig. 4. Palisades augite. (a) Termination of triple-chain zippers in augite. (b) Pervasive nucleation of short, doubly-terminated triple-chain zippers in augite.

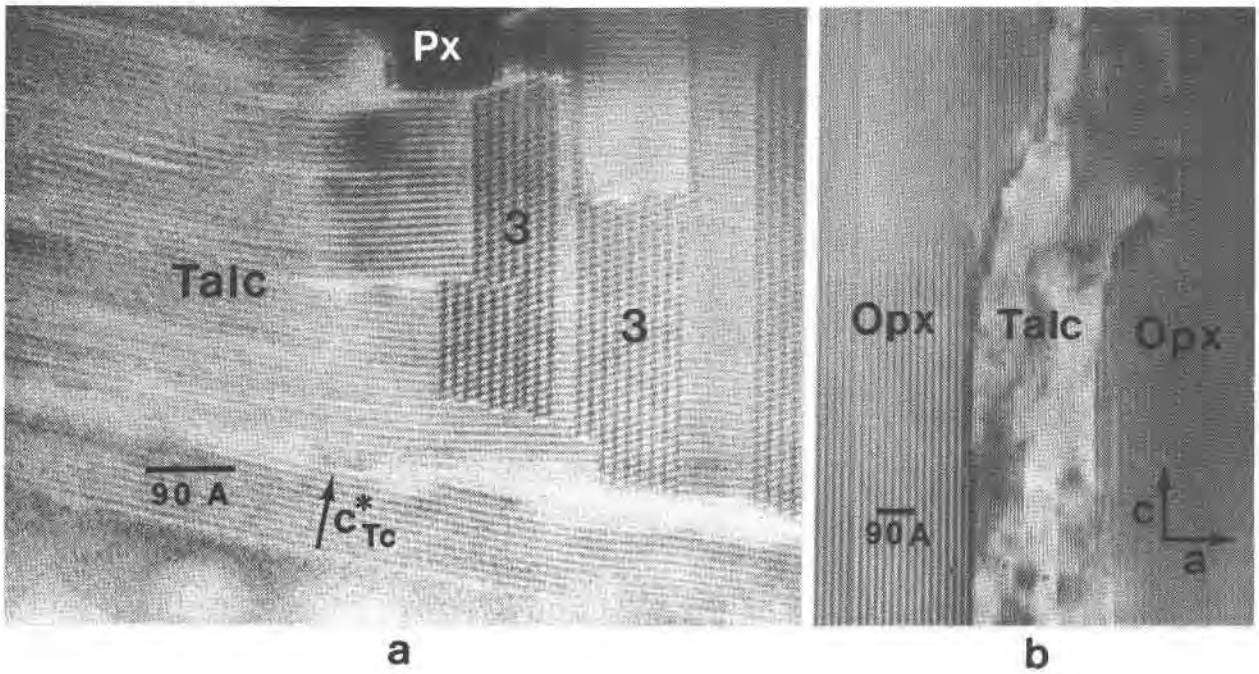

Fig. 5. Palisades augite. (a) Complex intergrowth of pyroxene, talc, and triple-chain silicate ("3"). (b) Direct replacement of orthopyroxene by talc along a fracture.

such as these are typical of the microstructures associated with hydration reaction of amphiboles at Chester, Vermont (Veblen and Buseck, 1980), suggesting that some of the amphibole in the Palisades augite is also reacting toward a mica or talc structure.

There is clearly a fascinating variety of microstructures associated with hydration reaction in this pyroxene specimen. The textures suggest that along fractures, pyroxene can react first to triple-chain silicate, which in turn transforms to talc or a mixture of talc and lizardite (planar serpentine). Alternatively, pyroxene can react directly to sheet silicate. Some of the amphibole in this specimen

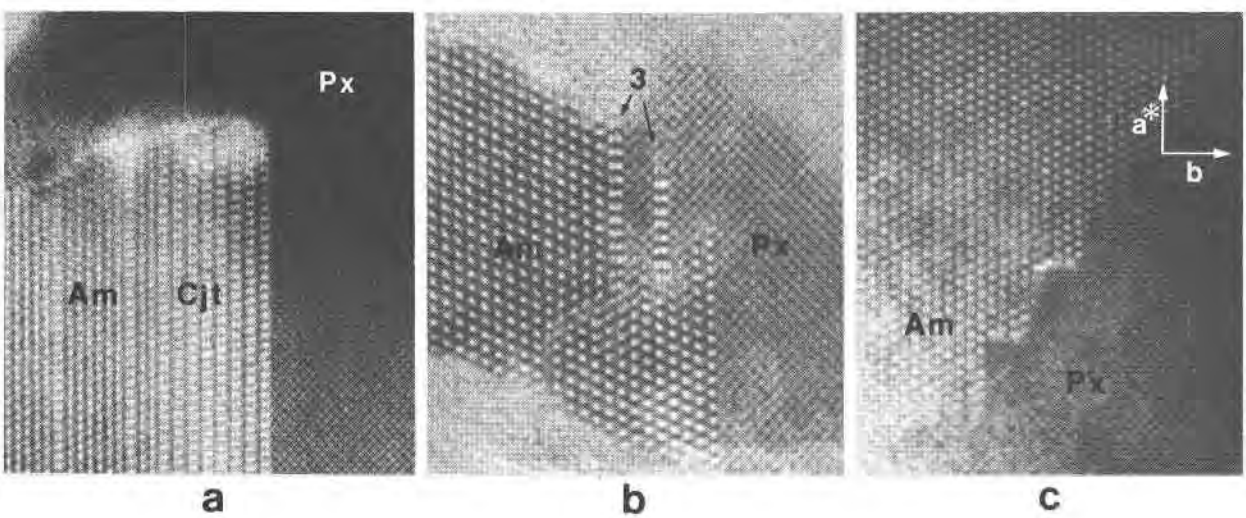

Fig. 6. Palisades augite. (a) Intergrown amphibole and triple-chain silicate (clinojimthompsonite—Cjt) replacing pyroxene near a fracture. (b) Amphibole and augite together with only limited amounts of triple-chain structure ("3"). (c) The boundary between an amphibole bleb and host augite. The two pyriboles share common crystallographic axes, but the boundary is irregular.

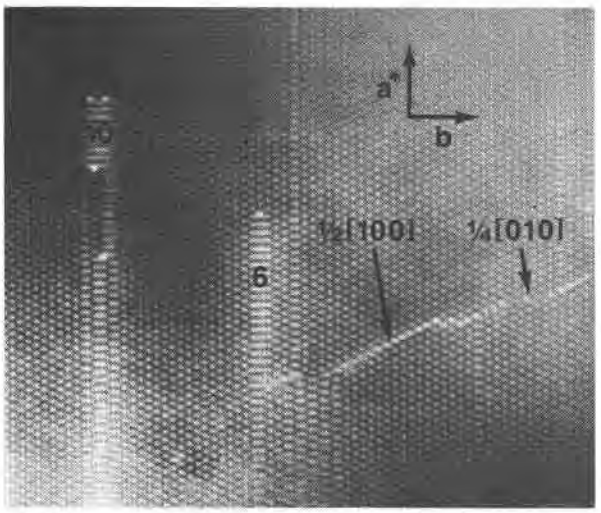

Fig. 7. Palisades augite. Part of an amphibole bleb showing wide-chain zippers and displacive faults typical of amphiboles undergoing reaction to sheet silicate. Zippers with chain widths of 6 and 10 are labeled.

appears to have grown from pyroxene with associated triple-chain silicate along a reaction front. The mode of formation of amphibole blebs in the pyroxene is, however, unresolved.

Salt Lake Crater augite

This clinopyroxene, which occurs in a pyroxenite nodule from Salt Lake Crater, Hawaii, contains rods and lamellae of clinoamphibole that are visible with a petrographic microscope. The thinner lamellae, which are less than a micron in width, are parallel to (010), whereas the larger lamellae have uneven boundaries and form a continuum with still larger amphibole rods (Fig. 8a), which are parallel to *c* and in some cases also roughly elongated in the *b* direction. This texture suggests that fine coherent amphibole lamellae first formed parallel to (010), but then broke coherence with the pyroxene structure and assumed non-planar boundaries once they reached a certain size. Although the distribution of amphibole lamellae generally appears to be random, in places the lamellae are obviously related to cleavage traces in the pyroxene (Fig. 8b). This texture strongly suggests that the amphibole formed as the result of alteration along a fracture, rather than by exsolution from the pyroxene.

Examination in the TEM has shown that in this specimen, unlike the Harzburg and Palisades specimens, there are no extremely fine amphibole or wide-chain lamellae. The widths of the finest lamellae appear to be in the tenth-micron range. One possible explanation for this lower size limit is that physical conditions changed after a period of amphibole nucleation; no new nuclei formed, while the existing lamellae grew to their present sizes. Another possibility is that smaller amphibole lamellae were at one time present in the sample; changing conditions could have increased the interface energies, leading to dissolution of the smaller lamellae. A third possibility is that the amphibole lamellae in this specimen initially grew as wide lamellae, and

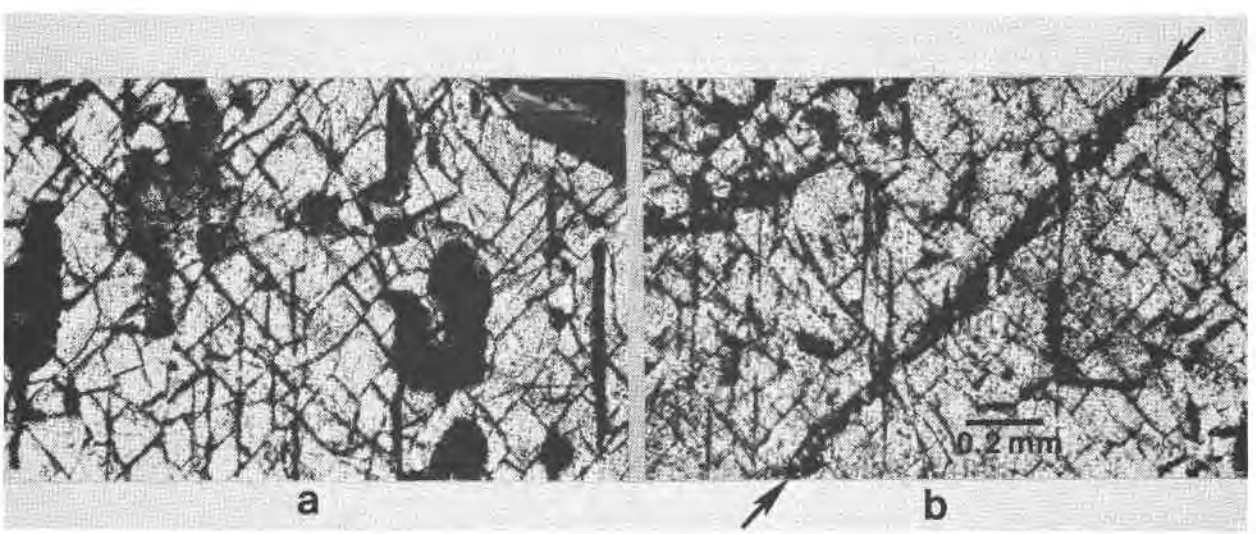

Fig. 8. Salt Lake Crater augite. Thin sections cut normal to *c* as viewed in plane polarized light; the (110) cleavage of the pyroxene is evident, and *b* is horizontal. (a) (010) lamellae of amphibole (dark vertical streaks) and amphibole rods (dark patches). (b) Growth of dark amphibole lamellae along a pyroxene cleavage trace, which runs from upper right to lower left (arrowed). This texture is suggestive of amphibole formation by alteration along a fracture in the pyroxene.

extremely fine lamellae were never present. The microstructures observed in this specimen do not elucidate the growth processes of the lamellae. They do, however, provide a striking contrast with the microstructures in specimens containing extremely thin lamellae of hydrous biopyriboles.

Figure 9a is an electron diffraction pattern from part of an amphibole lamella and some adjacent pyroxene. The diffractions are sharp, unlike those in the Harzburg intergrowths (Fig. 1), because there is no fine-scale intergrowth of pyroxene and amphibole. One important feature of this pattern is that a^* for the two reciprocal lattices is different, indicating that the spacing $(100)_{am}$ is nearly 1% larger than $(100)_{px}$. For a perfectly coherent (010) intergrowth of two different pyriboles, their (100) spacings should be nearly equal. This is, in fact, the case for the Harzburg intergrowths (Fig. 1) and finely intergrown pyriboles from Chester, Vermont (Veblen and Buseck, 1979a; lattice parameters from Veblen and Burnham, 1978a, for unconstrained macroscopic single crystals indicate a difference in (100) spacing of only 0.2% between anthophyllite and jimthompsonite). The (010) amphibole–pyroxene interface energy in the Salt Lake Crater augite is thus expected to be relatively high.

HRTEM images of the pyroxene–amphibole interfaces reveal numerous ledges. Some of these ledges obey the pyribole replacement rules (Veblen and Buseck, 1980), but most do not. Figure 9b shows two interface ledges. The white-arrowed ledge is two amphibole chains wide, while the black-arrowed ledge, which is accompanied by strain contrast, is only one amphibole chain wide; this ledge violates replacement rule 2, because one amphibole chain (an odd number) replaces two pyroxene chains (an even number). Such violations are also the sites of partial dislocations with displacements of ½[100] in the pyroxene structure; either partial or unit dislocations with displacements in this direction are necessary to accommodate the mismatch in amphibole and pyroxene lattice parameters described above. Insertion of ledges that are one amphibole chain in width permits the creation of dislocations with the smaller displacement, which may account for the abundance of single-width ledges. A few unit dislocations, unaccompanied by ledges, have also been observed in the interfaces. Figure 9c is an overview of one of the interfaces, with white and black arrows as in Figure 9b.

The pyroxene–amphibole interfaces in this specimen clearly exhibit far less coherence than the analogous (010) interfaces in the pyroxenes from Harzburg and the Palisades Sill and in the pyriboles from Chester, Vermont. Presumably the lesser coherence is a reflection of the greater mismatch in lattice parameters. The higher energy associated with a (010) interface of this sort probably led to readjustment of boundary orientations for the larger lamellae, resulting in the amphibole rods that are

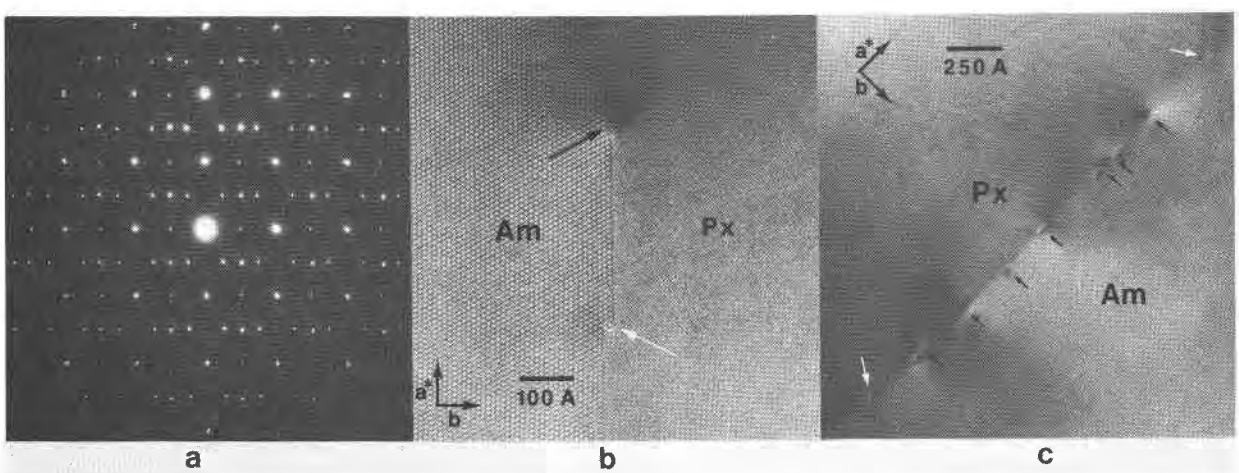

Fig. 9. Salt Lake Crater augite. (a) c-axis electron diffraction pattern with a^* vertical and b^* horizontal. Both amphibole and pyroxene diffractions are sharp (compare with Fig. 1a), and there is a difference of about 1% in a^* of the pyroxene and amphibole. (b) A pyroxene–amphibole interface showing a ledge two amphibole chains wide (white arrow) and a ledge one amphibole chain wide (black arrow). Strain contrast accompanies the ledge one chain wide. (c) An overview of a pyroxene-amphibole interface with ledges that violate the pyribole replacement rules (black arrows) and ledges that obey them (white arrows). The violating ledges are accompaneid by strain contrast.

present in this specimen. The pyroxene–amphibole interfaces of these rods are similar to the boundaries of the amphibole blebs in the Palisades augite (Fig. 6c).

Another feature of the Salt Lake Crater specimen is the presence of fractures in the amphibole that appear to have opened up in the *a* direction (Fig. 10a). These cracks typically terminate at or near the pyroxene–amphibole interface (Fig. 10b) and appear to represent tensional features in the amphibole. One possibility is that they were created during cooling or decompression. The mean thermal expansion coefficient of tremolite is more than twice that of diopside, for example (Cameron *et al.*, 1973; Sueno *et al.*, 1973), suggesting that the amphibole lamellae probably contracted more upon cooling than the pyroxene. This differential contraction could have resulted in the tensional cracks in the amphibole. Decompression would be expected to have the opposite effect from that of cooling and would not produce the observed fractures.

Roberts Victor Al-clinopyroxene

This high-alumina pyroxene from a grospydite nodule in the Roberts Victor kimberlite, South Africa, was shown on the basis of microprobe analyses to have a very high concentration of octahedral vacancies (Smyth, 1977, 1980; Smyth and Hatton, 1977). It is therefore thought to be a natural example of nonstoichiometric pyroxenes that have been grown in the laboratory at high pressures (O'Hara and Yoder, 1967; Wood and Henderson, 1978; Gasparik and Lindsley, 1980). The pyroxene is white, and in petrographic thin section it is nearly opaque. Within a petrographic microscope, the thin edges of ion-thinned specimens can be seen to consist of a vermiform intergrowth of two or more phases on a scale of less than a micron; it is presumably scattering by this fine intergrowth that leads to the non-transparency of the pyroxene. Using single-crystal X-ray methods, Smyth (1977, 1980) showed that the pyroxene grains consist of two pyroxenes plus fine-grained quartz.

This pyroxene was examined with HRTEM to determine whether or not some of the apparent nonstoichiometry resulted from primary intercalated amphibole or wide-chain silicate. Alternatively, condensation of vacancies during decompression could have resulted in the formation of oxyamphibole (or hydroxyamphibole, if water were permitted to enter the structure). A simplified form for such a vacancy-condensation reaction is

$$\underset{\text{(pyroxene)}}{4M_{1.75}\square_{0.25}(Si,Al)_2O_6} \rightarrow \underset{\text{(oxyamphibole)}}{M_7(Si,Al)_8O_{24}}$$

where □ refers to a vacancy, and M represents octahedral cations. In practice, the pyroxene would contain fewer vacancies than the above component, and the vacancies would diffuse to the growing amphibole lamellae.

Electron microscopy demonstrates that the above type of reaction did not occur pervasively in the Roberts Victor clinopyroxene; only a few amphibole lamellae were observed. All of these were only one amphibole chain wide (Figure 11), and hence violate the second coherent replacement rule. Terminations of the lamellae are associated with strain contrast. HRTEM of the specimen was

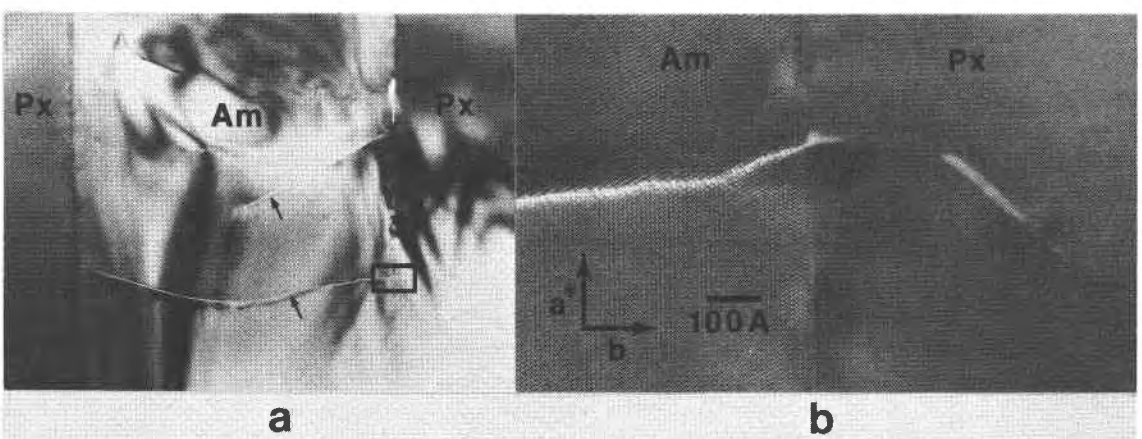

Fig. 10. Salt Lake Crater augite. (a) An amphibole lamella about 0.9 μm wide, showing tensional fractures (arrowed). (b) An enlargement of the boxed region in "a," showing termination of the fracture near the pyroxene–amphibole interface.

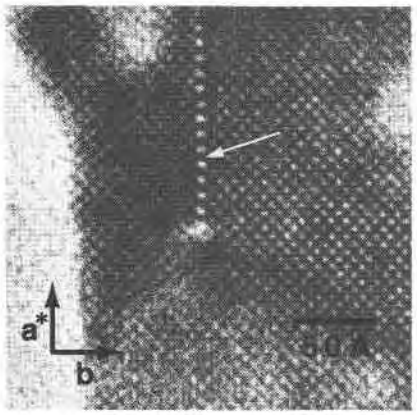

Fig. 11. Roberts Victor Al-clinopyroxene. Termination of an amphibole lamella one chain wide (arrowed) in pyroxene. Structural distortion and strain contrast accompany the termination.

difficult because the pyroxene suffered extremely rapid electron beam damage, in contrast to the behavior of most pyroxenes.

Although amphibole was not found in appreciable amounts, abundant sheet silicate was observed intergrown with the pyroxene in some parts of the specimen. The (00l) fringe spacings suggest that this material is, at least in part, mixed-layer chlorite–talc intergrowths. Some of this sheet silicate occurs as inclusions with planar boundaries parallel to (110), (100), and (010) of the pyroxene (Fig. 12). These inclusions may be analogous to the "flying saucers" reported in pyriboles from Chester, Vermont (Veblen and Buseck, 1980). The abundance of sheet silicates in this grospydite pyroxene indicates that substantial alteration has taken place. Care should therefore be exercised in the interpretation of analytical results, because it is conceivable that mixtures of pyroxene and certain sheet silicates could produce analyses characteristic of high-vacancy pyroxene alone. On the other hand, it is likely that the conclusions of Smyth (1977, 1980), based on electron microprobe analyses, are correct, because the distribution of sheet silicates in the specimen is quite inhomogenous. However, far more work will have to be done, preferably with analytical TEM methods, before the microstructures and distribution of phases in this complex specimen are fully understood.

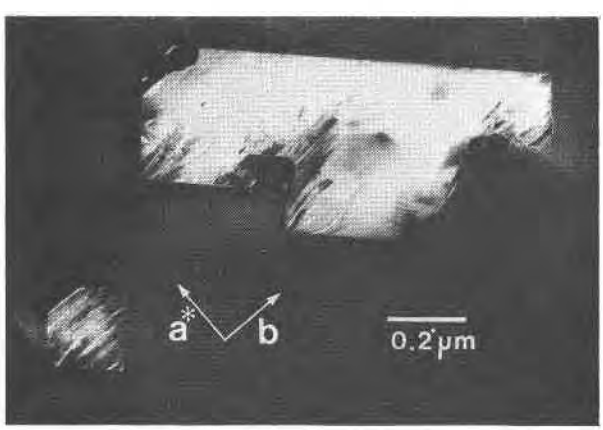

Fig. 12. Roberts Victor Al-clinopyroxene. Two inclusions of sheet silicate show preferred orientation of the interfaces parallel to pyroxene (110). Shorter stretches of interface can also be seen to parallel (100) and (010).

Pyroxenes mostly or completely replaced by other minerals

Loch Raven tremolite after diopside

This specimen is an obvious pseudomorph consisting of tremolite after pyroxene. In petrographic thin section, it appears to consist of a mixture of homogeneous tremolite and fine-grained quartz, and TEM examination confirms that these are the major minerals present. The tremolite contains extremely rare single- and triple-chain lamellae that are one chain wide (Fig. 13). Low-angle grain boundaries are a common feature in the amphibole. These boundaries are primarily structurally coherent, with dislocations spaced every few hundred to few thousand Ångströms. In some cases, the dislocation spacing is much closer, and parts of the boundary suffer spots of rapid electron beam damage (Fig. 14). This unusual behavior could be related to destabilization of the structure near the dislocations.

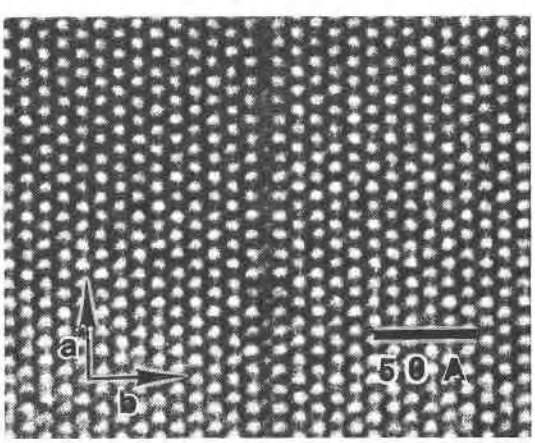

Fig. 13. Loch Raven tremolite after diopside. A chain-width error consisting of a slab one pyroxene chain wide runs vertically in the center of the figure.

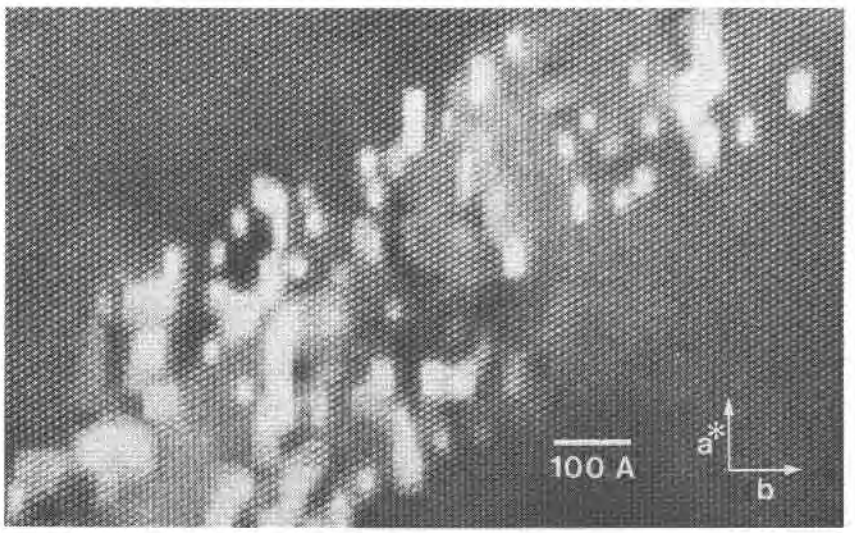

Fig. 14. Loch Raven tremolite after diopside. A low-angle grain boundary in tremolite with numerous partial dislocations and unusual contrast.

One inclusion of remnant pyroxene was observed in this specimen, surrounded by quartz. The inclusion is 5 μm across, and diffraction patterns and HRTEM images show it to be perfectly ordered pyroxene, in the same orientation as the amphibole in the specimen. It is possible that this armored inclusion survived without reacting to tremolite because it was surrounded and protected by quartz. Because no other remnant pyroxene was observed, the pyroxene–amphibole textural relationships could not be determined, and it is therefore not possible to draw direct conclusions about the hydration mechanisms in this case. However, less direct evidence for the mechanisms will be discussed in the section "Polysomatic Out-of-Phase Boundaries."

White Picacho spodumene

This spodumene specimen has undergone partial hydrothermal alteration to a micron-scale intergrowth of albite, eucryptite, and muscovite (London, 1979). HRTEM revealed no structural abnormalities in the pyroxene, although the muscovite exhibits extreme stacking disorder. The reaction is thus a structurally simple heterogeneous replacement reaction, with no associated coherent replacement of the pyroxene by hydrous biopyriboles. The lack of such replacement may be related to the fact that there are no Li–Al clinoamphiboles analogous to spodumene, and octahedral cations other than Al may not have been present in high enough concentrations to form clinoholmquistite; pyroxenes of other compositions might show very different behavior when placed in the same environment.

Copper Mountain uralite

Amphibole and pyroxene. The Copper Mountain uralite bears the clear morphology of pyroxene. Electron microscopy shows that almost the entire specimen has been converted to amphibole, although there are rare remnant patches of pyroxene. These patches have no consistent or clearly defined shape; a typical boundary between pyroxene and amphibole is shown in Figure 15a. The boundary is apparently not parallel to the pyribole c-axis, and the unusual contrast in the boundary region results from the overlapping of amphibole and pyroxene structures in the image. This overlapping also results in multiple diffraction, which causes the amphibole and pyroxene $h + k =$ odd diffractions to appear in Figure 15b (the pyriboles are both C-centered, so that these reflections are electron-forbidden and do not appear in electron diffraction patterns from areas of non-overlapping structure). The amphibole–pyroxene c-axis diffraction pattern of Figure 15b contrasts sharply with that of Figure 9a, which is from an intergrowth in which the pyroxene–amphibole interface is parallel to the viewing direction.

No defects have been observed in the remnant pyroxene in this uralite, except in the immediate neighborhood of the pyroxene–amphibole boundaries, indicating that the pyroxene → amphibole reaction mechanisms in this case did not rely on the

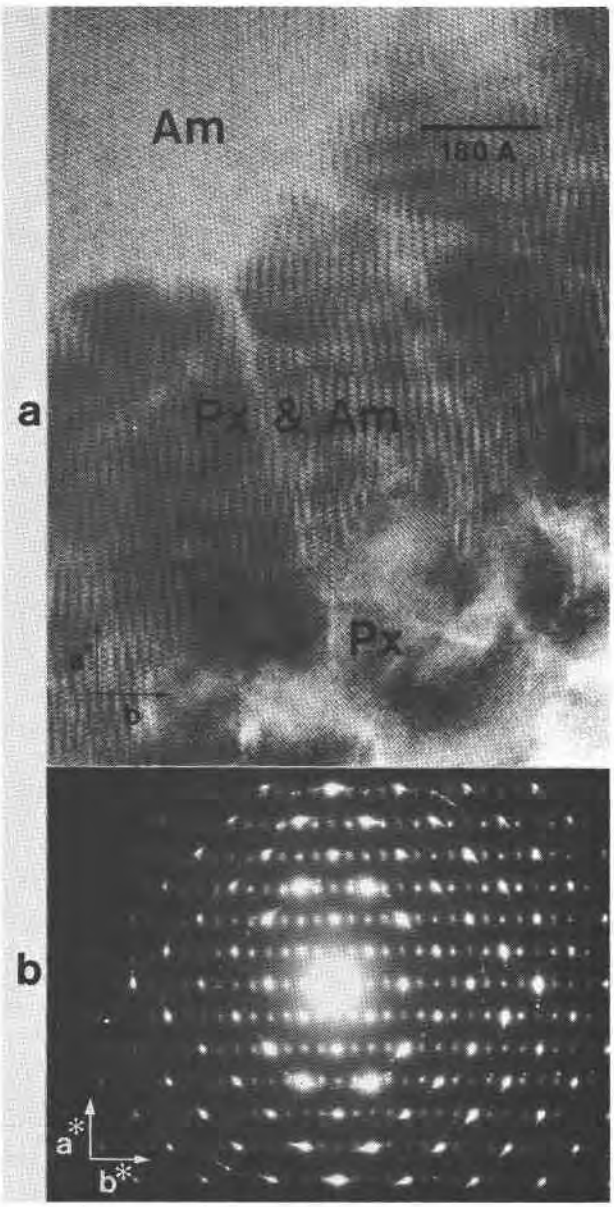

Fig. 15. Copper Mountain uralite. (a) A typical boundary between amphibole and remnant pyroxene. The unusual contrast of the boundary region results from overlapping of the pyroxene and amphibole structures, similar to a Moiré image. (b) *c*-axis electron diffraction pattern showing multiple diffraction resulting from overlapping of the pyroxene and amphibole structures (compare with Figure 9a).

growth of double- or triple-chain zippers. Instead, conversion to amphibole appears to have taken place by bulk transformation along a reaction front that moved through the crystal. Orientation relationships were retained between the parent and daughter chain silicates. The HRTEM images also show that the transformation took place in such a way that either the left or right half of every amphibole I-beam (when viewed with *b* horizontal) assumed the position of an I-beam in the original pyroxene structure. In places, double- or triple-chain zippers are observed to extend a short distance into the pyroxene from the pyroxene–amphibole boundary, but these zippers are uncommon and are always limited in extent. They are therefore probably not important for the bulk transformation mechanism.

Rare single-, triple-, and quadruple-chain lamellae occur parallel to (010) in the amphibole of this specimen (Fig. 16). These chain-width errors are invariably only one silicate chain wide, and in places there is anomalous contrast in the surrounding amphibole, possibly resulting from strain (Fig. 16a). The lamellae extend for long distances through the amphibole, and some are offset by displacive faults (Fig. 16b and the triple-chain error in Fig. 16a). These lamellae are discussed in the section "Polysomatic Out-of-Phase Boundaries."

In addition to the extended chain-width errors described above, zippers of many different chain widths occur in amphibole near fractures that are filled with sheet silicates. We interpret these zippers as resulting from hydration of the amphibole subsequent to its formation from pyroxene. In places, numerous very short, doubly-terminated wide-chain zippers occur close to sheet silicate (Fig. 17). These, again, are presumably related to late-stage hydration of the amphibole along fractures. Silicate chains of anomalous width have also been observed in low-angle grain boundaries that are nearly parallel to (010). For example, the amphibole domains on the left and right sides of Figure 18 are in slightly different orientations. Structural continuity is maintained by changing the chain width on the boundary from single, to quadruple, to triple.

Sheet silicates. As noted above, the Copper Mountain uralite contains sheet silicates that are apparently the result of reaction between amphibole and fluids along fractures. Electron microscopy of fine-grained sheet silicates such as these is difficult, because they suffer rapid beam damage, and proper orientation of the small crystals is important. Structural interpretation of HRTEM images of randomly-oriented grains can be very risky, because the pattern of the (00l) fringes can change drastically with changes in orientation. Fortunately, the sheet silicates in the two uralites examined in this study tended to form with their sheets parallel to the

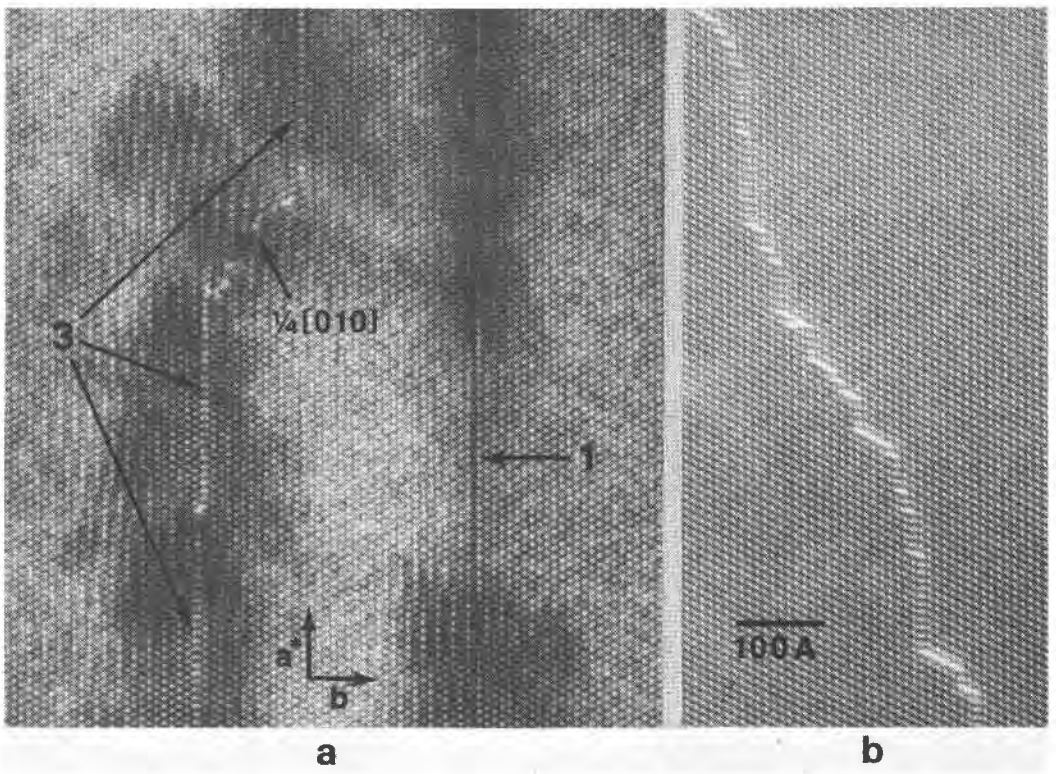

Fig. 16. Copper Mountain uralite. (a) Triple ("3") and single ("1") chain-width errors in amphibole. The triple-chain error is offset by faults having projected displacements of ¼[010]. (b) A quadruple chain-width error that is offset in numerous places by faults with projected displacements of ½[100].

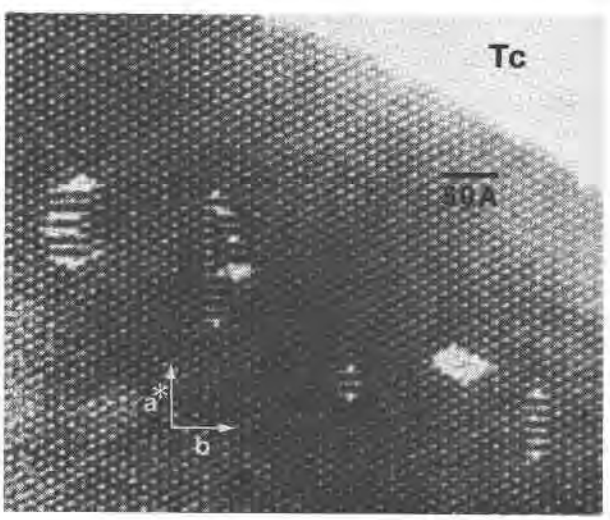

Fig. 17. Copper Mountain uralite. Short, double-terminated zippers of wide-chain silicate growing in amphibole near a grain boundary filled with talc. Two of the zippers are simple, consisting purely of sextuple-chain material, while the other two are complex, consisting of silicate with double, triple, and wider chains.

silicate chains of the host pyribole. Thus, orientation of the amphibole *c*-axis parallel to the electron beam automatically resulted in the proper orientation for high-resolution imaging of the sheet silicate (00l) planes. In addition, the presence of amphibole in most of the sheet silicate images permitted excellent internal magnification calibration. It is these circumstances that allow the reliable structural interpretation of (00l) fringes in fine-grained sheet silicates, as used by Veblen and Buseck (1979b).

Chlorite, talc, and lizardite are all present in this specimen. Figure 19a shows these three minerals occurring together within a space of a few dozen Ångströms. In addition to areas where they form discrete domains, as in Figure 19a, talc and chlorite in places intergrow freely on (00l), forming a disordered mixed-layer silicate that has a range of structural formulae that are chemically collinear between those of chlorite and talc. Individual talc and brucite-like layers commonly terminate (Fig. 19b,c). The rare intercalation of 5Å sheets in talc has

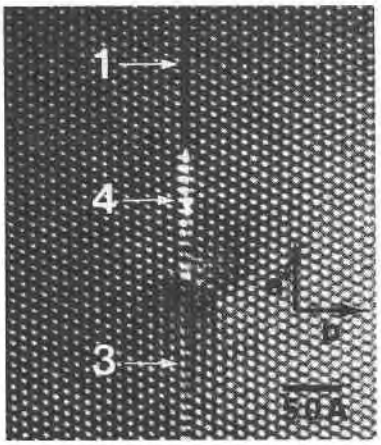

Fig. 18. Copper Mountain uralite. A low-angle grain boundary separating two amphibole domains parallel to (010). The structural misfit is accommodated by distortion and changing of the chain width of the boundary from single ("1") to quadruple ("4") to triple ("3").

previously been reported from Chester, Vermont (Veblen and Buseck, 1980). Figure 19d shows an example of chlorite intergrown with amphibole. Presumably the chlorite layers that terminate in the amphibole formed by growth along the sheet edges at the expense of the chain silicate.

Romanian uralite

Amphibole. This uralite from Ocna de Fier, Romania, has been completely converted to clinoamphibole and sheet silicates and is finely intergrown with calcite. In some areas, the amphibole possesses perfect chain-width order; electron diffraction patterns contain sharp $h + k$ = odd diffractions, indicating that the amphibole is primitive (Fig. 20a). The amphibole therefore probably has a low calcium content, but this could not be confirmed with the electron microprobe because of the intimate intermixture with calcite.

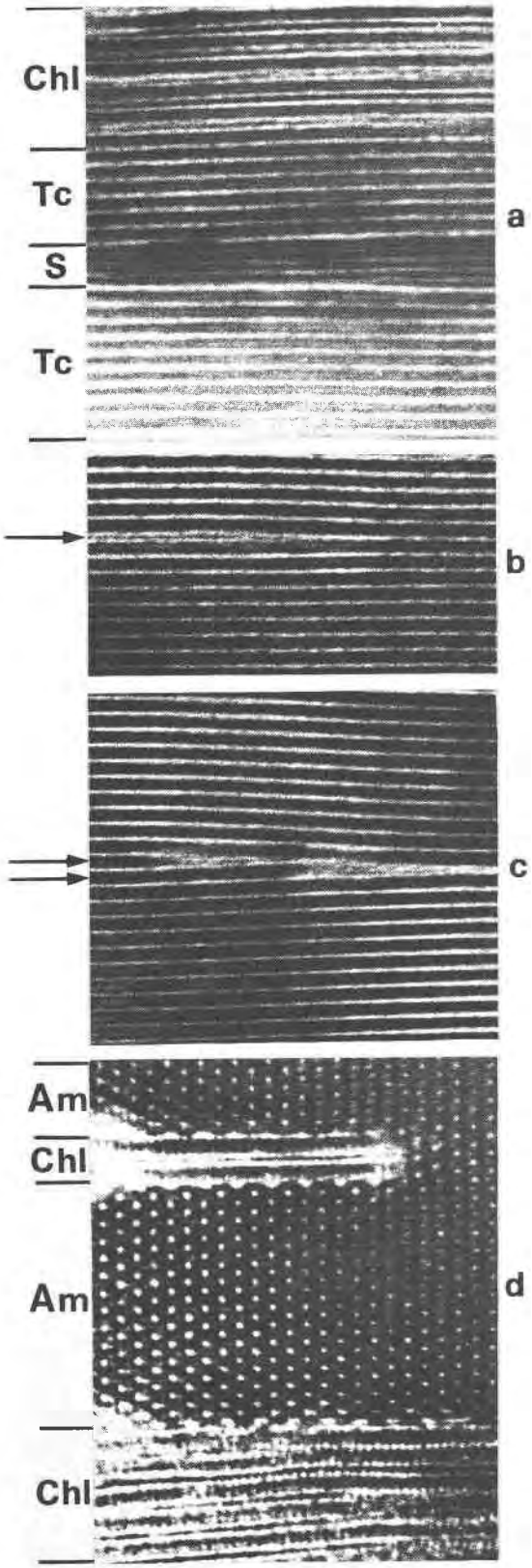

Fig. 19. Copper Mountain uralite. Sheet silicates intergrown on (001); c^* is vertical, and fringe spacing in the talc regions is 9.3Å. (a) Intergrowth of chlorite, talc, and planar serpentine structures. (b) Intercalation and termination of a 5Å brucite layer (arrowed) in talc. The intercalation is structurally equivalent to the insertion of one layer of chlorite structure. (c) The termination by dislocation of two talc layers (arrowed). (d) Chlorite intergrown with amphibole. A short chlorite sequence consisting of talc–brucite–talc layers terminates in the upper portion of the figure.

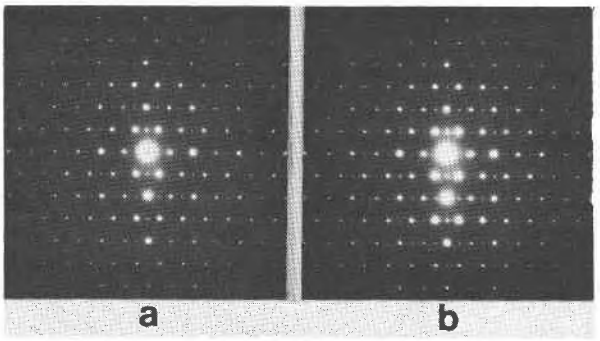

Fig. 20. Romanian uralite. (a) Electron diffraction pattern of structurally-ordered clinoamphibole showing primitive $h + k =$ odd diffractions. b^* is horizontal. (b) Diffraction pattern from chain-width disordered region, showing light streaking parallel to b^*.

Most of the amphibole contains moderate numbers of triple, quadruple, and quintuple chain-width errors, with triple chains predominating. Diffraction patterns from these areas show the characteristic streaks parallel to b^* (Fig. 20b). In addition to these nearly pervasive wide-chain lamellae, there are also patches of zippers having even wider chains that are associated with the edges of amphibole grains in contact with sheet silicates; this is similar to the situation in the Copper Mountain uralite. These areas show features that are typical of hydrating amphiboles (Veblen and Buseck, 1980).

Sheet silicates. Much of the amphibole in this specimen has been replaced by talc, serpentine, and chlorite, some of which is very finely intergrown on (001). Some of the structural aspects of these intergrowths and of the combination planar and roll structures in the serpentine have been discussed by Veblen and Buseck (1979b). Areas that contain both amphibole and sheet silicates commonly produce electron diffraction patterns such as that shown in Figure 21. This pattern contains a great deal of information. The sharp diffractions arise from the amphibole (Am). Weak $h + k =$ odd diffractions and light streaking parallel to b^* indicate that the amphibole is primitive and possesses minor chain-width disorder. The (00l) diffractions from talc (Tc) and serpentine (S) are arcuate, indicating rotational disorder about the direction of the amphibole c axis. Diffuse intensity occurring between the talc and serpentine (00l) diffractions indicates that the talc and serpentine structures are finely intergrown. The other arcuate regions of intensity to the left and right of the center of the diffraction pattern are (hkl) diffractions from the serpentine and talc, again showing the effects of misorientation. Perhaps most important, this diffraction pattern shows that the sheet and chain silicates are oriented so that the talc and serpentine sheets are parallel to the amphibole chains. Therefore, when the amphibole in this specimen has been oriented with its c-axis parallel to the electron beam, the sheet silicates are also in perfect orientation for imaging their (00l) fringes. Because of this orientation relationship, there are no ambiguities in the imaging conditions for HRTEM, and the interpretation of the images is straightforward.

The intergrowth of talc, serpentine, and chlorite in this Romanian uralite is similar to that in the Copper Mountain uralite (Fig. 19a, b), except that chlorite is much less abundant. Serpentine is concentrated near the amphibole; farther from the amphibole, the only sheet silicate is talc. Figure 22 shows part of a curious region observed in talc, in which the sheets are pulled apart to form a cellular structure. This has not been observed in other specimens; the texture could have been produced either by tensional deformation, perhaps during sample preparation, or by partial dehydration during ion milling.

The most interesting of the sheet silicates is the serpentine. Chrysotile, lizardite, and antigorite all occur in this specimen, and much of the serpentine consists of intergrowths of both planar (lizardite) and roll (chrysotile) forms; two excellent examples

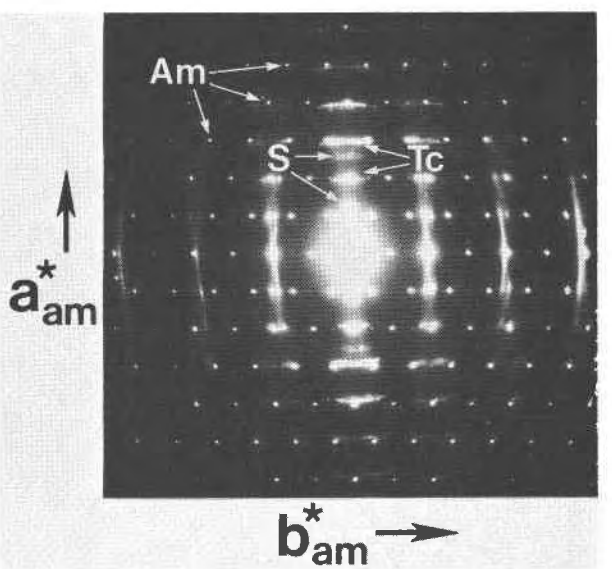

Fig. 21. Romanian uralite. Electron diffraction pattern of a complex amphibole(Am)–talc(Tc)–serpentine(S) intergrowth. See text for explanation.

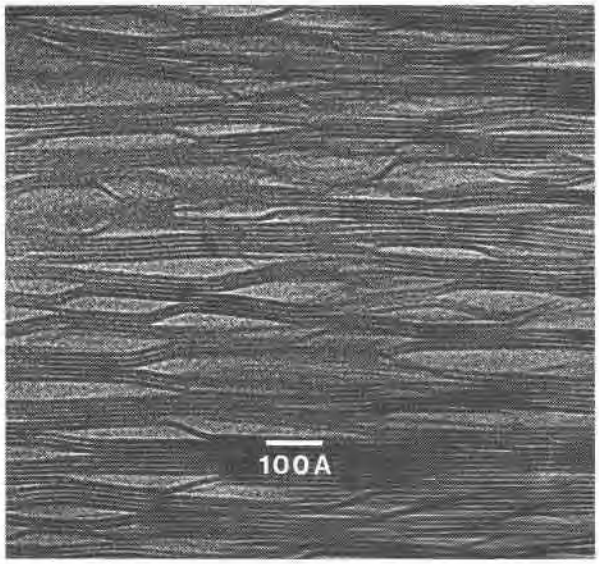

Fig. 22. Romanian uralite. Cellular structure in talc. The sheets are partially pulled apart, possibly as an artifact of sample preparation.

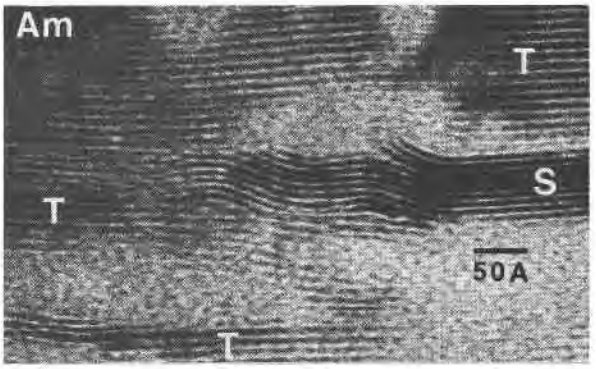

Fig. 24. Romanian uralite. Combination of planar and curved forms of serpentine (S), intergrown with talc (T) and amphibole (Am). Curvature reversals result in an undulating serpentine structure with a wavelength of about 150Å, much longer than the typical antigorite wavelength.

of such intergrowths were shown in Figure 2 of Veblen and Buseck (1979b). A different example is in Figure 23, which shows talc, serpentine, and amphibole occurring together. The serpentine contains both planar and curved areas, which combine to form a braided pattern; reversal of curvature direction occurs in some sheets. Figure 24 shows similar reversals combining to form an undulating structure, along with planar serpentine, talc, and amphibole. The wavelength of the undulations is about 150Å, which is longer than the wavelength typical of antigorite. A problem that is raised by these reversals in the sense of curvature is that the structure at the point of reversal could be expected to be the same as that at the reversals in antigorite. It is expected that at least slight offset of the (00*l*) fringes should occur at the curvature reversal, as shown by Yada (1979), but the layers in these serpentines generally appear to be completely continuous through the reversal. Future imaging calculations might help to explain why this offset is not always observed.

In the complete chrysotile rolls that have been observed in this specimen, the (00*l*) fringes are never seen to cross; this is consistent with the interpretation that these complete rolls form long fibers parallel to the axis of curvature. Fibers with both concentric cylindrical layers and layers that are rolled up like a carpet have been observed, similar to the observations of Yada (1967, 1971) in commercial quality chrysotile asbestos. In regions where planar and roll forms of serpentine combine, however, the basal fringes are frequently seen to cross each other, as shown in Figure 25. Because the TEM specimen thickness is less than about

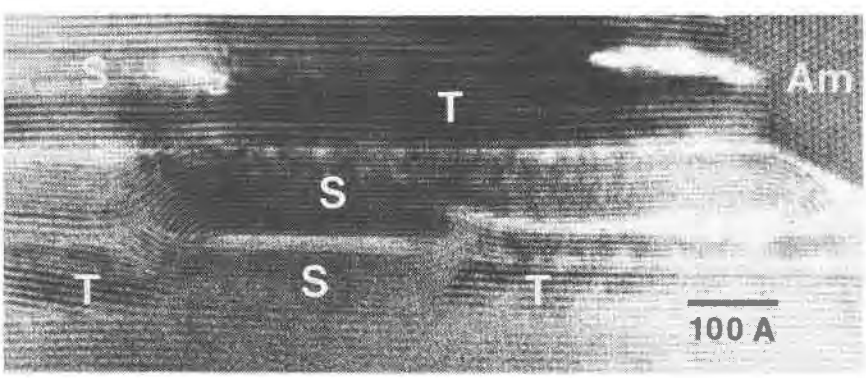

Fig. 23. Romanian uralite. Braided pattern of planar and curved serpentine (S) intergrown with talc (T) and amphibole (Am). Some serpentine layers exhibit reversal of the sense of curvature.

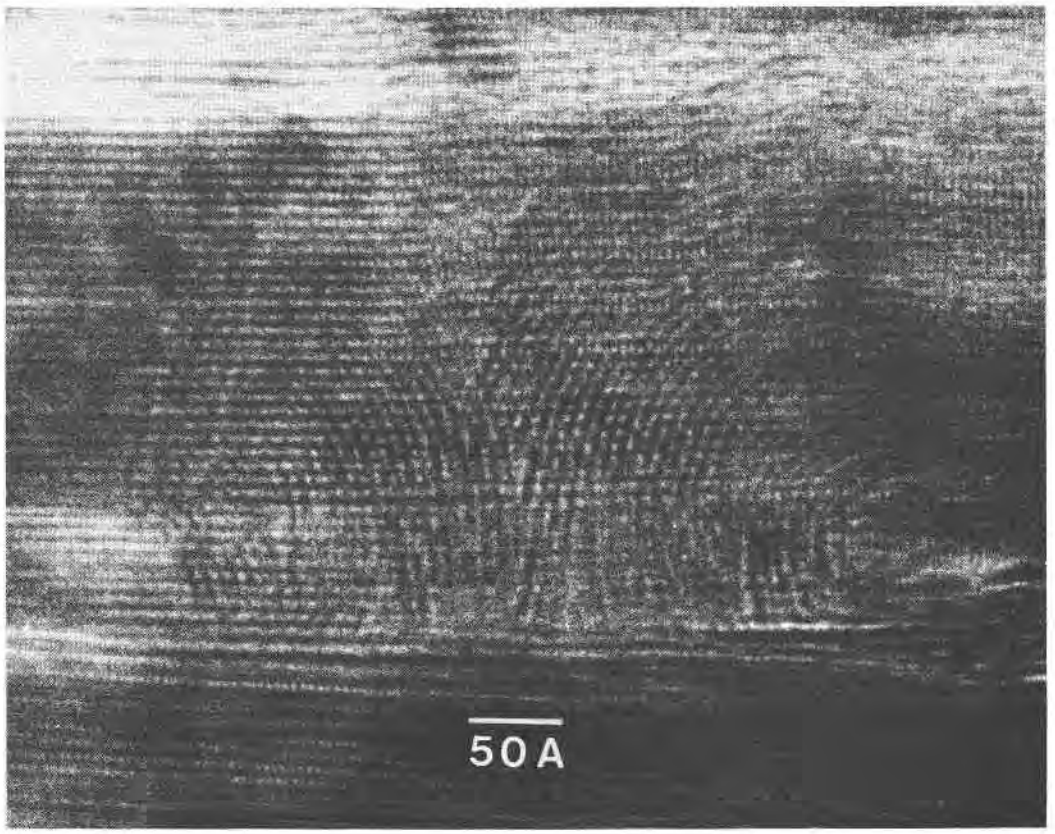

Fig. 25. Romanian uralite. Crossing of (001) fringes from planar and curved serpentine. Features such as this suggest that the serpentine is a ribbon structure, as shown in Figure 26.

100Å, this overlapping indicates that individual serpentine layers are not very extensive in the direction of the curvature axis. Instead of forming layers up to several centimeters in extent in this direction, as in some chrysotile asbestos, the layers in the combination planar and roll serpentine form ribbons. A qualitative model of what this type of serpentine might look like is sketched in Figure 26.

The width of the serpentine ribbons can be roughly estimated by observing that in regions of planar-roll combination structure, roughly five to fifteen percent of the area contains overlapping fringes. If the average TEM specimen thickness is around 50Å, this suggests that the average ribbon width is around 500Å. In any case, it is clear that this type of serpentine is best viewed as a ribbon structure. Similar ribbon structures are known from other systems, most notably some kinds of graphitized carbon (Jenkins and Kawamura, 1976). A drawing of one of these structures, as derived by Ban *et al.* (1975), is shown in Figure 27.

Reaction mechanisms

The description of a reaction mechanism in a solid state system is dependent on the scale at which the reaction is observed. With a petrographic microscope, for example, it might be possible to determine whether a replacement reaction occurs by the formation of macroscopic lamellae or by bulk conversion along a broad reaction front. On the scale observable with HRTEM, more details of the reaction mechanism can be determined; for example, in the case of the Harzburg orthopyroxene, we know that amphibole formed by a mechanism involving the growth of lamellae and lamellar ledges two amphibole chains wide. We therefore understand the reaction mechanism on a scale of a few Ångtröms. However, we still do not know any details of the mechanism on an atomic scale. No experimental method now available can tell us exactly how individual atoms are moving during solid state reactions in chain silicates. It is, howev-

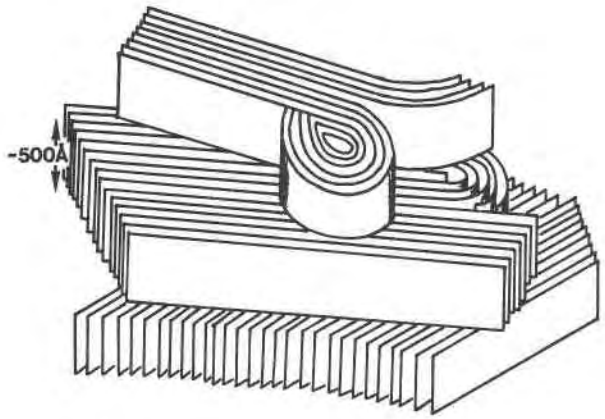

Fig. 26. An idealized sketch of the ribbon structure of the combination planar-roll serpentine in the Romanian uralite. The viewing direction in the electron microscope is vertical.

er, possible to speculate on such atomic movements.

Ribbe and Nakajima (1980) have suggested a detailed, atom-by-atom mechanism for the transformation of the silicate chains in pyroxene to double, triple, or wider chains. This simple mechanism only requires atomic movements less than 2Å. However, Ribbe and Nakajima neglect the important role that octahedral cations play in these reactions. In order to convert a slab of pyroxene structure three chains wide into a zipper of triple-chain material one chain wide, for example, it is necessary not only for some octahedral cations to diffuse out of the crystal, but also for at least one-sixth of the pyroxene octahedral cations to pass *through* the (100) tetrahedral layers (in calcic pyroxenes, incompatibility of Ca with the regular ocahedral sites of the triple-chain structure requires still more cations to pierce the tetrahedral layers). It is very difficult to see how the mechanism of Ribbe and Nakajima can operate in reality, given these requirements for redistribution of octahedral cations. Furthermore, experimentally determined structures of the terminations of sextuple-chain slabs in amphibole (Veblen and Buseck, 1980) indicate that the tetrahedral layers do *not* remain intact during the analogous hydration reaction in amphibole, as would be required by the mechanism of Ribbe and Nakajima. At present, we believe that polysomatic reactions in biopyriboles can be understood on the scale observable with HRTEM. Speculative discussions of the mechanisms on a smaller scale (Eggleton, 1975; Veblen and Buseck, 1980; Ribbe and Nakajima, 1980) raise important questions of crystal chemistry, but the assignment of exact motions to specific atoms during such reactions is premature. Accordingly, in the following discussion of reaction mechanisms, we have restricted ourselves to the scale observable with HRTEM.

The pyroxene reaction mechanisms that operated in the specimens described above can be classified into at least five categories:

1. Invasion of the pyroxene by narrow lamellae (zippers) of amphibole having an even number of amphibole chains (Harzburg orthopyroxene).
2. Invasion of pyroxene by zippers of triple-chain silicate one chain wide (Palisades augite).
3. Bulk oriented conversion of pyroxene to amphibole, triple-chain silicate, or disordered pyribole along a reaction front (Copper Mountain uralite, Palisades augite).
4. Bulk conversion of pyroxene or secondary amphibole to a mixture of minerals, such as sheet silicates, showing a variety of orientation relationships (White Picacho spodumene, Roberts Victor Al-clinopyroxene, Harzburg orthopyroxene, Palisades augite, both uralites).
5. Mechanisms that can no longer be determined because the critical textures characteristic of the reaction have been erased or are not recognized (Salt Lake Crater augite, Loch Raven tremolite after diopside).

Reaction paths observed in these specimens and in pyriboles from Chester, Vermont (Veblen and Buseck, 1979a, 1980) are summarized in Figure 28;

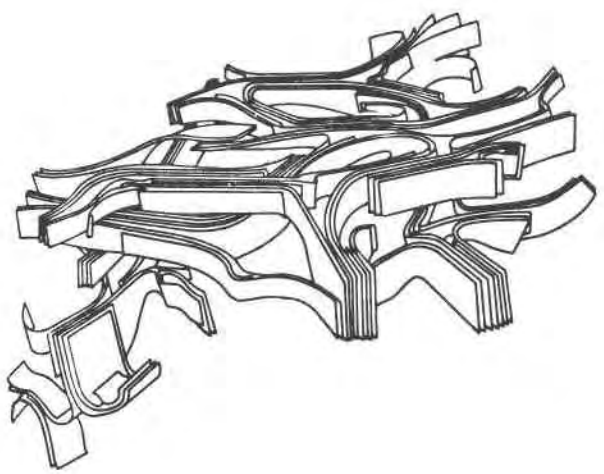

Fig. 27. The ribbon structure of a polymerized carbon (*Ban et al.*, 1975). This type of ribbon structure differs from that in Figure 26 in that the axes of layer curvature are not restricted to a single direction.

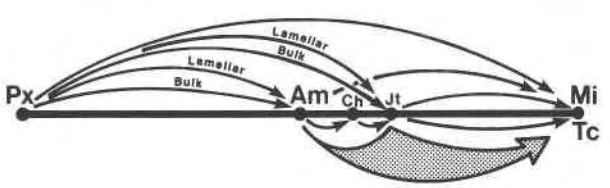

Fig. 28. Summary of observed reaction paths for pyribole alteration. The paths above the Pyroxene–Mica (or Talc) join represent specimens in the present paper, and those below the join represent mechanisms at Chester, Vermont (Veblen and Buseck, 1980). The two discreet compositions shown to the right of amphibole are chesterite and jimthompsonite.

paths that involve minerals that are not biopyriboles are not included.

Several generalizations can be made about these reaction schemes. Most obviously, there are several ways by which a pyroxene can hydrate. Not only can different mechanisms result in different reaction products (double- or triple-chain material, for example, in cases 1 and 2), but also the same reaction product can result from different mechanisms (amphibole can be formed either by zipper growth or by bulk replacement along a reaction front, as in cases 1 and 3; also, sheet silicates can apparently form either by direct replacement of pyroxene or by reaction from an intermediate product, such as amphibole). This multiplicity of reaction paths and mechanisms is similar to the behavior noted for the hydration of amphiboles at Chester, Vermont. Thus, in both pyroxene and amphibole hydration, there are apparently complex relationships among the reaction mechanisms, the reaction path, the identity of the final product phases, and the structures of the reactant phase and product phases.

Interpretation of the reaction paths and products in terms of compositional differences and environmental parameters, such as thermal regime of alteration, is thwarted by the paucity of data. Indeed, there are marked differences in reaction behavior among all the specimens examined, and there are clearly reaction types that we did not examine, such as the reaction of pyroxene to (100) amphibole lamellae (Desnoyers, 1975; Yamaguchi *et al.*, 1978; David Bish and Charles W. Burnham, personal communication). Until many more specimens of each type have been examined or controlled reaction experiments have been combined with electron microscopy, it will not be possible to rigorously relate reaction categories with other parameters. However, we can identify a few factors that are undoubtedly important controls on hydration behavior.

The first important factor is the compositions and resultant equilibrium cell parameters of the host and product chain silicates. Just as in the case of pyroxene and amphibole exsolution lamellae, strain energies arising at the intergrowth interfaces will control the orientation of lamellae as outlined by the exact phase boundary theory (Robinson *et al.*, 1971, 1977; Jaffe *et al.*, 1975). Where there is strong control of orientation by structural constraints, as in the case of very narrow zippers of amphibole or triple-chain silicate in pyroxene, the interface strain energies conversely might constrain the chemistry of lamellae at compositions uncharacteristic of bulk equilibrium. Furthermore, the interface strain energies might well control the identity of the product structure in cases where the bulk free energies of two possible products are close. For example, even if bulk amphibole were more stable than a bulk triple-chain structure, narrow lamellae with clinojimthompsonite structure might be more stable in intergrowth with pyroxene, if the interface strain energies were lower than those associated with narrow amphibole lamellae. As another example, the energies of numerous narrow lamellae with coherent interfaces might in some cases exceed the energy of a randomly-oriented incoherent interface, leading to bulk replacement along a reaction front, rather than a lamellar replacement mechanism.

Another important factor controlling reaction behavior is probably the thermodynamic stability relationships. For example, it might be that a clinojimthompsonite structure type is more stable than amphibole when alteration takes place in a sheet silicate stability field. The thermodynamic stabilities may couple with strain considerations, as discussed above, to determine the identity of the reaction product in lamellar replacement. Kinetic factors are also likely to be important. When the rate of bulk replacement along a front is faster than that of replacment by narrow zippers, the bulk replacement mechanism will predominate. The kinetics of the reacting system might also be strongly coupled with the stability relationship: if a pyroxene is well into the amphibole stability field, where the pyroxene–amphibole free energy difference is large, rapid replacement along an incoherent front might be favored, whereas the rate for coherent zipper replacement might exceed that of bulk replacement when the energy difference is smaller. The notion

that two different mechanisms having different rates may compete with each other is strengthened by observations on the Copper Mountain uralite, where amphibole zippers uncommonly extend into pyroxene from the replacement front; both mechanisms operated, but the bulk replacement mechanism clearly predominated in this case. On the other hand, bulk replacement by disordered pyribole apparently took place along the grain boundaries of the Harzburg orthopyroxene, but, in this case, the predominant mechanism was the more rapid pervasive replacement by narrow amphibole zippers. In still other specimens, such as the Palisades augite and the augite of Nakajima and Ribbe (1980), there is evidence for several different modes of reaction. It is not known whether these different types represent different stages in the alteration history, or whether they were all competing with each other at one time.

Exsolution versus hydration reaction

Papike *et al.* (1969) considered four possible ways to derive pyroxene–amphibole intergrowths: (1) alteration (hydration reaction) of pyroxene, (2) exsolution, (3) prograde rection of amphibole, and (4) primary epitaxial growth of pyroxene and amphibole. In most of the cases considered here, there is textural and other evidence that rules out possibilities (3) and (4) (they cannot explain why the amphibole lamellae in the Harzburg orthopyroxene always contain an even number of chains, for example). Furthermore, the extent of reaction demonstrates unquestionably that uralites form by hydration reaction of pyroxene. The question that remains is whether intergrowths of amphibole and triple-chain lamellae in pyroxene were produced by hydration alteration or by exsolution from pyroxenes having solid solution toward amphibole compositions.

Constraints on the nucleation and growth of polysomatic zippers in pyroxene are the same whether the zippers form by an exsolution (isochemical) or alteration (diffusional) process. It is therefore not possible to determine directly which process is operating, because amphibole lamellae with even widths or triple-chain lamellae one chain wide, for example, should result in either case. In determining which process produces narrow lamellae in pyroxene, it is therefore necessary to rely on indirect chemical and textural arguments.

Desnoyers (1975) and Smith (1977) argued that the marked difference in chemistry (increased alkalis and aluminum in the amphibole lamellae) was inconsistent with an alteration origin. It has since been shown, however, that growing zippers in chain silicates have large tunnels at their terminations (Veblen and Buseck, 1980), and rapid diffusion of cations in and out of the structure along these channels probably does not impose serious constraints on alteration reactions. The compositions of coarse-grained amphibole coexisting with similar pyroxenes show that increased Na and Al is to be expected in equilibrium amphibole lamellae. The chemical relationships observed by Smith and Desnoyers between lamellae and host are therefore quite consistent with an alteration origin in which there is diffusion not only of water, but also of cations, in and out of the crystal. Yamaguchi *et al.* (1978) presented compositional profiles across an amphibole lamella; the profiles showed depletion in the pyroxene near the lamella of those elements in which the lamella was enriched (Al), and enrichment in those elements that were lower in the lamella (Si and Ca). Yamaguchi *et al.* argued that these depletions and enrichments are evidence for an exsolution origin. At the same time, however, they cited evidence that the formation of the lamellae occurred at a lower pressure than the primary crystallization of the pyroxene. Lower pressure would favor lower Na and Al and increased Si and Ca in the equilibrium pyroxene composition. The observed compositional profiles could therefore be explained as the result of reequilibration of the pyroxene in the neighborhood of the amphibole lamellae, where diffusion could occur during zipper growth. Furthermore, amphibole that is clearly produced by alteration and forms rims on the pyroxene of Yamaguchi *et al.* is chemically very similar to the lamellar amphibole. This similarity is to be expected if the pyroxene acted as an open system, at least in the locations of amphibole lamella growth. However, the similarity would be coincidental if there were no diffusional communication between the crystal interiors, where exsolution would take place, and the rims, where hydration reaction occurred.

It is clear from the above that neither alteration nor exsolution reaction has been ruled out on chemical grounds as the cause of fine amphibole lamellae intergrown with pyroxenes; both mechanisms are consistent with the analytical observa-

tions of Desnoyers (1975), Smith (1977), and Yamaguchi *et al.* (1978). Textural arguments may therefore be the best means of determining the mechanism. Of the specimens examined in this study, it is clear from the completeness of reaction and pseudomorphic shapes that the tremolite after diopside, the spodumene, and the two uralites reacted by an alteration mechanism; the high-Al clinopyroxene also shows evidence of extensive local alteration, although it is not clear what mechanism accounted for the rare amphibole lamellae. The Palisades augite also clearly reacted by hydration, since reaction is localized at fractures, and the production of narrow lamellae of hydrous biopyriboles is typically followed by complete alteration to sheet silicates.

The Harzburg orthopyroxene and Salt Lake Crater augite are thus the only specimens in which amphibole may have been produced by exsolution. The textures of the Harzburg specimen again suggest an alteration origin: the orthopyroxene crystals are rimmed by sheet silicates and very wide-chain pyribole that clearly formed by alteration, and the amphibole lamellae appear to be more abundant near the grain boundaries. There is no detectable alteration near the centers of the larger orthopyroxene grains (P.P.K. Smith, personal communication). This is the pattern that would be expected from alteration, with amphibole zippers nucleating at the grain boundaries, but it is also possible that this texture could have been produced by the combination of amphibole exsolution from a zoned crystal and hydration along the crystal rim.

The Salt Lake Crater augite contains the most interesting textures observable with the petrographic microscope and is perhaps the most important specimen because the textures closely match most of those described by Desnoyers (1975) and Yamaguchi *et al.* (1978) in specimens that they interpreted as examples of amphibole exsolution. Yet, as described earlier, the amphibole lamellae in one part of the Salt Lake Crater specimen are obviously related to a cleavage trace in the pyroxene (Fig. 8b), strongly suggesting a hydration reaction origin for the amphibole. Furthermore, in some parts of this specimen there is simply too much amphibole to have exsolved from any reasonable pyroxene composition. The microstructural evidence combined with the petrographic textures suggest that there is an evolutionary continuum between the fine amphibole lamellae and the large amphibole rods and blobs. These considerations again point to an origin by alteration, rather than exsolution.

In summary, we do not believe that chemical considerations exclude either exsolution or alteration as possible mechanisms of formation for amphibole lamellae in pyroxenes. The textures in all of the specimens examined in this study indicate that hydration reaction is the most likely mechanism, and similarities among textures observed in the present work and in studies by others suggest that alteration may account for the lamellae in most other cases as well. With the exception of a few specimens examined by Smith (1977), pyroxenes with amphibole lamellae have been reported only from rocks that also contain discrete grains of amphibole or other hydrous silicates that clearly arose by alteration. This association should arouse suspicion of an exsolution mechanism for the formation of hydrous pyribole lamellae in pyroxenes of any rocks that clearly have undergone hydration alteration.

Polysomatic out-of-phase boundaries

Antiphase boundaries are a common product of ordering reactions in widely diverse crystalline systems. They can result, for example, from atomic ordering in alloys (Fisher and Marcinkowski, 1961) or from displacive positional ordering in silicates (Morimoto and Tokonami, 1969). Antiphase boundaries can arise when two patches of the ordered phase originate in two different parts of the disordered crystal. If the two patches are not ordered in phase with each other, an antiphase boundary forms where they grow together. If the patches are in phase, no boundary is formed.

In theory, a similar but more complex mechanism exists for boundary formation during polysomatic replacement reactions. As an example, let us choose the replacement of pyroxene by amphibole along a reaction front. In all cases where pyroxene → amphibole has been observed, the amphibole I-beams form in positions such that one of the sides of each I-beam occupies the position of one side of a pyroxene I-beam in the parent structure. Stated differently, the M4 and T2 polyhedra on one side of the new amphibole I-beam occupy the former positions of an M2 and T polyhedron in the replaced pyroxene. Given this constraint, if there exists a patch of amphibole replacing a pyroxene crystal, and if a new patch nucleates, either within the

crystal or on its surface, there are not two, but four possible phase relationships between the two patches. These four possibilities are illustrated on the left side of Figure 29, where the bulk amphibole structure represents a patch that has already nucleated and grown in the parent pyroxene. The darkened amphibole I-beams that are isolated in the pyroxene structure represent the four different phase positions for the second nucleation event. Where the two patches completely replace the pyroxene and

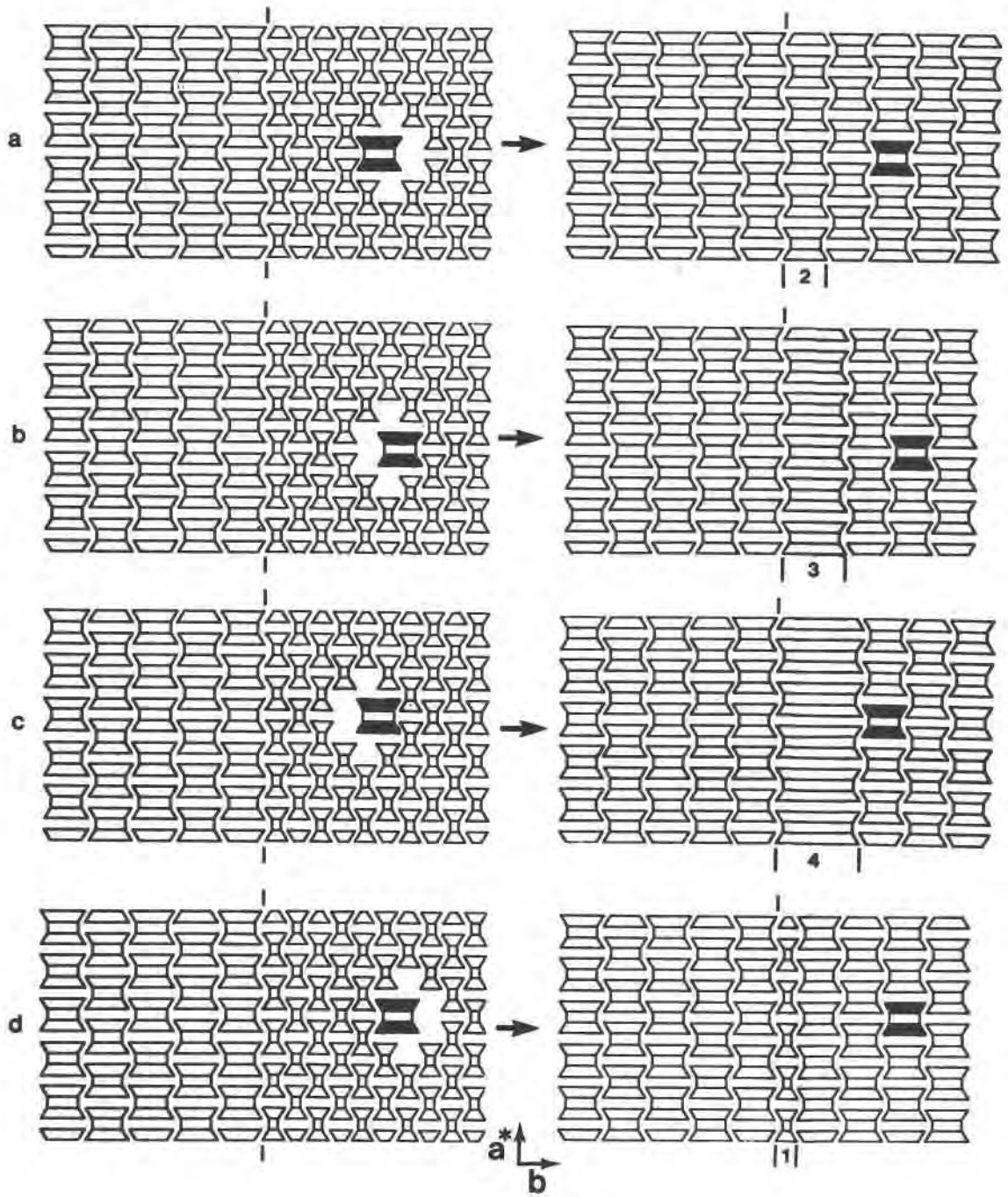

Fig. 29. Formation of polysomatic out-of-phase boundaries. Different phasing of nucleation events shown on the left results in different types of boundaries shown on the right, as follows: (a) No boundary. (b,c,d) triple, quadruple, and single chain-width errors, respectively.

have grown together, they form polysomatic boundaries, or chain-width errors, as shown on the right of Figure 29. In one case (a), the two patches grow together coherently, resulting in uninterrupted amphibole; in the other three cases, slabs of triple-, quadruple-, and single-chain silicate result, if the boundary is oriented parallel to (010). In other orientations, the boundaries would be displacive planar faults, as discussed in this paper and by Veblen and Buseck (1980).

The displacements on these faults would be ($\frac{1}{4}b + \frac{1}{2}c$), $\frac{1}{2}b$, and ($-\frac{1}{4}b + \frac{1}{2}c$) for cases b, c, and d of Figure 29 respectively, where b and c are amphibole axes. Because the boundaries arising from this multiple nucleation mechanism are not all out of phase by π (antiphase), because their structures are simply those of polysomatic defects when oriented parallel to (010), and because they arise by replacement of one member of a polysomatic series by another, we refer to them as "polysomatic out-of-phase boundaries." These boundaries separate "polysomatic out-of-phase domains."

We can now ask whether or not polysomatic out-of-phase boundaries arise in nature during replacement reactions. This is not a simple question, because such boundaries are structurally identical to the single, triple, and quadruple chain-width errors that could arise as defects during primary crystal growth or during reaction by cooperative zipper growth. There is therefore no rigorous way to prove whether or not the chain-width errors in a given sample arose by nucleation and growth of polysomatic out-of-phase domains, or by other mechanisms. There are, however, some suggestive characteristics in the distribution of chain-width errors that can be predicted to arise from a domain nucleation and growth process. First, we would expect to see single, triple, and quadruple chain-width errors in greater abundance than other widths (with the exception noted below, where quintuple-chain errors replace the single-chain mistakes). This contrasts with the distribution in anthophyllite that has experienced partial reaction by zipper growth at Chester, Vermont (Veblen and Buseck, 1980); in that occurrence, sextuple zippers are more abundant than quadruples and quintuples, and single-chain errors are absent. Immediately following replacement of a pyroxene crystal by nucleation and growth of amphibole, the numbers of single, triple, and quadruple chains should be equal because the probabilities of nucleation in each of the three out-of-phase positions are presumably equal. Subsequent annealing could, however, selectively remove the less stable widths by the migration of partial dislocations, for example (see Figure 4a, b in Veblen and Buseck, 1980). As a result, the numbers of single, triple, and quadruple errors need not be equal when observed in the electron microscope. It further might be expected that polysomatic errors arising from a domain nucleation mechanism would be fairly evenly distributed throughout an amphibole crystal, rather than clumped togeher. In the Chester occurrence, on the other hand, wide-chain zippers tend to be clumped, while very large areas of the ordered phases remain perfectly ordered. Polysomatic out-of-phase boundaries would not be expected to be concentrated near grain boundaries, as are zippers resulting from amphibole hydration in some specimens.

If we examine the distribution of chain-width errors in the Copper Mountain uralite, we find that there are a few single-, triple-, and quadruple-chain slabs scattered through the specimen (Fig. 16). Most of these mistakes are spaced far apart, although some are quite close to others (Fig. 16a). Fewer quadruple-chain errors were observed than single- and triple-chain errors, but the numbers of mistakes observed are low enough so that the difference in frequency may not be significant. The distribution of polysomatic defects is at least consistent with the hypothesis that they arose by independent nucleation of out-of-step amphibole domains in the pyroxene. These chain-width defects are in general quite continuous in the (010) plane, although some of them are offset by displacive faults. It is possible that initially the domains were more equant, and that they elongated parallel to (010) during annealing. This is logical, because the displacive faults presumably have higher energies than chain-width errors and would hence tend to be selectively removed during annealing; such a process would result in the observed tendency of the boundaries to be parallel to (010).

At first glance, the chain-width errors in the Romanian uralite appear to be inconsistent with formation by multiple nucleation of out-of-phase amphibole domains in the primary pyroxene. For example, triple-chain lamellae are much more common than quadruple and quintuple errors, there are no single-chain mistakes, and the quintuple-chain slabs that are present in the specimen are not explained by the simple domain model described

above. However, the over-abundance of triple-chain errors might be explained by assuming that the other types of polysomatic boundaries were selectively removed during annealing, or that there was an additional mechanism by which triple-chain slabs were produced. Furthermore, a slight modification of the polysomatic out-of-phase domain model for boundary formation can easily explain the absence of single-chain errors and the presence of quintuple-chain defects. As shown in Figure 30, the phase difference between two amphibole domains is the same when the domains are separated either by a single-chain slab or a quintuple-chain slab. In cases where a single-chain polysomatic out-of-phase boundary is quite unstable, it is therefore possible that a quintuple-chain boundary will form instead. In place of single-, triple-, and quadruple-chain boundaries, we would find triple-, quadruple-, and quintuple-chain boundaries. This is what is observed in the Romanian uralite. As in the Copper Mountain uralite, the sextuple zippers that form by zipper nucleation and growth during amphibole hydration are absent, except very close to grain boundaries. It is quite possible, then, that in both cases at least some of the chain-width errors in the amphibole formed by the nucleation and coalescence of out-of-phase amphibole domains. It is also possible that the few single- and triple-chain errors that were observed in the pseudomorph of tremolite after diopside arose in the same way. The extreme rarity of the chain-width errors in this specimen could indicate either a very low amphibole nucleation rate compared to the growth rate or annealing subsequent to reaction that efficiently eliminated the boundaries. Quadruple chains may not have been observed simply because not enough material was examined or because they were selectively annealed out.

The formation of polysomatic out-of-phase boundaries by independent nucleation events as described in this section may not be restricted to the case of amphibole replacing pyroxene. The theory is, in fact, quite general and will hold for any material undergoing reaction from one polysome to another by a nucleation and domain-growth mechanism. It has been suggested that such a mechanism could be responsible for polysomatic defects in humite group minerals that have been artificially heated (Butler, 1972), and it may be that similar polysomatic defects arise during reactions in the full range of minerals having polysomatic structures.

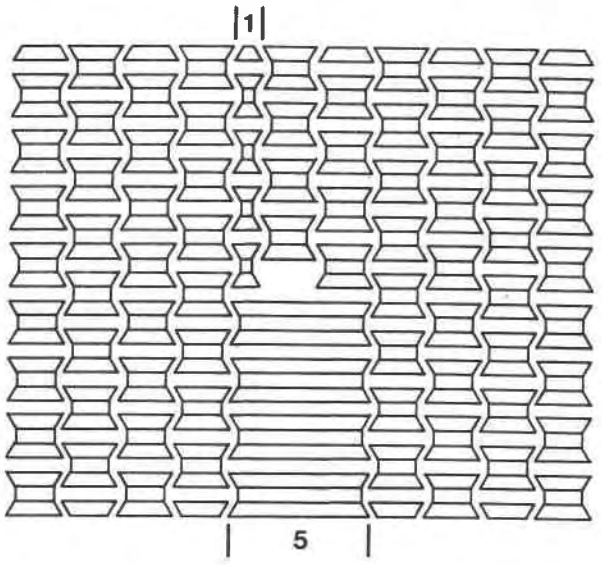

Fig. 30. Two amphibole domains out of phase by $-\frac{1}{4}b + \frac{1}{2}c$. The displacement between the two domains is the same whether they are separated by a single-chain slab (top) or a quintuple-chain slab (bottom).

Cation partitioning in polysomatic intergrowths: a geothermometric example

Many geochemical methods that are used in igneous and metamorphic petrology rely on the cation partitioning behavior of minerals. Studies in which these partitioning characteristics are crucial include investigations of trace element distributions and determinations of temperatures and pressures by a variety of methods. As almost universal constituents of lower crustal and upper mantle rocks, pyroxenes have been utilized in a wide variety of these geochemical schemes, and it is therefore prudent to ask whether they are always suitable for the application of such methods. How much will polysomatic lamellae of amphibole or other hydrous biopyriboles in a pyroxene affect the partitioning behavior and therefore the reliability of partitioning methods? Are such lamellae absent in almost all pyroxenes of geochemical interest, or are abundant lamellae that are unresolvable in the petrographic microscope a common feature? It is not possible to answer the second question, because very few pyroxenes have been examined with appropriate electron microscopic techniques at this time. By making a few simple assumptions it is, however, possible to roughly evaluate the effect of amphibole lamellae in those cases in which they are present.

Let us assume that we wish to obtain a two-pyroxene temperature for a rock by analyzing the coexisting orthopyroxene and clinopyroxene (*a la* Boyd and Nixon, 1973). Let us further assume that we accidentally analyze a clinoamphibole instead of the clinopyroxene. We can obtain a very rough estimate of the amphibole composition that might coexist with a clinopyroxene by assuming that the regular octahedral sites in the amphibole (M1, M2, M3) would have the same occupancies as the regular site in the clinopyroxene (M1), and that the distorted octahedral sites (M4 in amphibole and M2 in pyroxene) will also have the same composition. Because all of the Ca enters the distorted octahedral sites, it follows that the amount of wollastonite component in the amphibole would be 4/7 of that in the coexisting clinopyroxene. If the clinopyroxene had a composition "Px" (Wo = 45%) as shown in Figure 31, then the clinoamphibole would have the apparent composition "Am," much higher up on the solvus. The temperature obtained by using the amphibole analysis in place of the pyroxene composition would be in error by several hundred degrees.

The above scenario is, of course, a fairy tale. The amphibole analysis would immediately be recognized as such because the analysis total would only be about 98% and because stoichiometry and charge-balance criteria would be inconsistent with a pyroxene structure. Furthermore, the orthopyroxene composition would not be a temperature match with the faulty "clinopyroxene" analysis, and the amphibole might contain more Na and Al than expected in the clinopyroxene. But what would happen if, instead of analyzing a pure pyroxene or a pure amphibole, we were to analyze a mixture of 90% pyroxene with 10% optically unresolvable amphibole lamellae? If our microprobe analysis were perfect, it would total 99.8%, which is respectable by any standard. When normalized to a pyroxene basis, the discrepancies in stoichiometry and charge balance would be minor (for an intergrowth restricted to the cations of the pyroxene quadrilateral, the cation sum would be low by only 0.025 per six oxygens). Even the most careful analyst might not recognize that there was anything wrong with the pyroxene.

The composition of the pyroxene–amphibole mixture would not be far from that of the ideal pure pyroxene; it would plot in the position marked "10%" in Figure 31. In terms of temperature, however, it would appear to be about 120° higher on the solvus than the pure pyroxene (Lindsley and Dixon, 1976). If one were not careful, the use of the pyroxene–amphibole intergrowth could thus result in a substantial error in temperature. Because the Wo content of the orthopyroxene is low, intergrowth with small amounts of orthoamphibole would not appreciably affect its Wo content. The petrologist might notice that something was wrong with his analysis because the clinopyroxene and orthopyroxene compositions do not fall at the same temperature, but this check might be overlooked because the low-Ca side of the solvus is much steeper than the high-Ca limb.

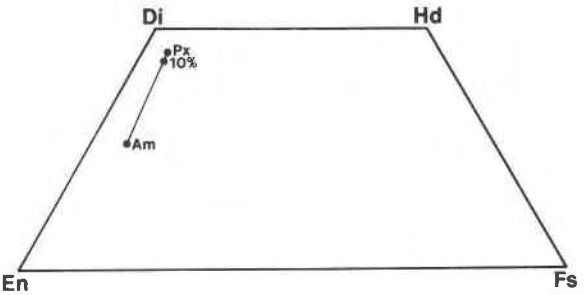

Fig. 31. Error introduced by analyzing pyroxene containing 10% amphibole lamellae, assuming theoretical cation partitioning behavior (see text).

The above example shows that substantial errors could, in fact, be introduced by polysomatic intergrowths in pyroxene when using geochemical methods relying on cation partitioning. Problems would occur not only in the simple case above, but also in any other geothermometric or geobarometric methods employing pyroxenes. It may be that optically unresolvable intergrowths are rare in pyroxenes and may therefore be ignored. The growing number of reports of hydrous biopyribole intergrowths in pyroxenes suggests, however, that they may be quite common, especially in high-pressure occurrences. Ideally, all pyroxenes used for geochemical investigations should be examined by a competent electron microscopist with a modern TEM capable of resolving polysomatic imperfections. In the years ahead, high-resolution TEM should prove to be a valuable petrologic tool, not simply from the petrographic standpoint, but also for the detection of defective minerals that should be avoided in geochemical studies.

Conclusion

No one of sound mind has ever suggested that the pyroxenes are a simple group of minerals. However, the specimens examined in this study demon-

strate unexpected complexities associated with pyroxene replacement reactions and with the microstructures that are produced by these reactions. In different circumstances, pyroxenes can react to amphibole, to triple-chain silicate, or to a variety of sheet silicates. For any given reaction path, there may be multiple mechanisms; for example, pyroxene can transform to amphibole in at least two different ways, and these different reaction mechanisms lead to different types of microstructures in the reaction products. In some cases, several types of reaction are observed in the same crystal. The final products of alteration typically consist of complicated intergrowths of several phases. The sheet silicates formed by reaction from pyroxene exhibit a wide range of structural variations, such as combinations of different structure types and mixed layering.

The factors that control the types of reaction behavior that occur in any given situation are poorly understood. Future experimental work may help to clarify the conditions under which different mechanisms operate, as well as the reaction kinetics. Although there are many unresolved problems, we know now that pyroxene replacement can occur on many different scales, and some pyroxenes that appear to be unaltered in thin section may, in fact, have undergone substantial replacement. This observation should not be lost on mineralogists and petrologists, since partially altered pyroxenes can behave very differently geochemically than those that are pristine.

Acknowledgments

Specimens employed in this study were kindly supplied by Drs. Arthur Boettcher, Donald Burt, David London, and Joseph Smyth and by the U. S. National Museum. We thank Mr. James Clark for performing the microprobe analyses, some of them on difficult material. The manuscript was improved by helpful reviews from Drs. Paul Ribbe and Maryellen Cameron. This research was supported by NSF grants EAR7927094, EAR7700128, and EAR7926375. Microscopy was performed in the Arizona State University Facility for High Resolution Electron Microscopy, which was established with support from the NSF Regional Instrumentation Facilities Program, grant CHE7916098.

References

Ban, L. L., Crawford, D. and Marsh, H. (1975) Lattice-resolution electron microscopy in structural studies of non-graphitizing carbons from polyvinylidene chloride (PVDC). Journal of Applied Crystallography, 8, 415–420.

Bown, M. G. and Gay, P. (1959) The identification of oriented inclusions in pyroxene crystals. American Mineralogist, 44, 592–602.

Boyd, F. R. and Nixon, P. H. (1973) Origin of the ilmenite–silicate nodules in kimberlites from Lesotho and South Africa. In P. H. Nixon, Ed., Lesotho Kimberlites, p. 254–268. Lesotho National Development Corporation, South Africa.

Buseck, P. R., Nord, G. L., Jr., and Veblen, D. R. (1980) Subsolidus phenomena in pyroxenes. In C. T. Prewitt, Ed., Pyroxenes, Mineralogical Society of America Reviews in Mineralogy, 7, p. 117–211.

Buseck, P. R. and Veblen, D. R. (1978) Trace elements, crystal defects, and high resolution electron microsopy. Geochimica et Cosmochimica Acta, 42, 669–678.

Butler, S. A. (1972) Breakdown Reactions in the Humite Mineral Group. Ph.D. Thesis, University of Cambridge, Cambridge, England.

Chisholm, J. E. (1973) Planar defects in fibrous amphiboles. Journal of Materials Science, 8, 475–483.

Chisholm, J. E. (1975) Crystallographic shear in silicate structures. In M. W. Roberts and J. M. Thomas, Eds., Surface and Defect Properties of Solids, Vol. 4, p. 126–151. The Chemical Society, London.

Desnoyers, C. (1975) Exsolutions d' amphibole, de grenat et de spinelle dans les pyroxenes de roches ultrabasiques: peridotite et pyroxenolites. Bulletin de Societe Francais de Mineralogie et Cristallographie, 98, 65–77.

Eggleton, R. A. (1975) Nontronite topotaxial after hedenbergite. American Mineralogist, 60, 1063–1068.

Fisher, R. M. and Marcinkowski, S. (1961) Direct observation of antiphase boundaries in the $AuCu_3$ superlattice. Philosophical Magazine, 6, 1385–1405.

Francis, D. M. (1976) Amphibole pyroxenite xenoliths: Cumulate or replacement phenomena from the upper mantle, Nunivak Island, Alaska. Contributions to Mineralogy and Petrology, 58, 51–61.

Gasparik, T. and Lindley, D. H. (1980) Experimental Study of pyroxenes in the system $CaMgSi_2O_6$–$Ca_{0.5}AlSi_2O_6$. (abstr.). Transactions American Geophysical Union (EOS), 61,402–403.

Isaacs, D., Brown, P. E., Essene, E. J. and Peacor, D. R. (1980) Pyroxene-amphibole intergrowths from a garnet granulite—exsolution or replacement? (abstr.). Geological Society of America Abstracts with Programs, 12, 453.

Jaffe, H. W., Robinson, P., Tracy, R. J., and Ross, M. (1975) Orientation of pigeonite lamellae in metamorphic augite: correlation with composition and calculated optimal phase boundaries. American Mineralogist, 60, 9–28.

Jenkins, G. M., and Kawamura, K. (1976) Polymeric Carbons. Cambridge University Press, Cambridge, England.

Lindsley, D. H. and Dixon, S. A. (1976) Diopside–enstatite equilibria at 850° to 1400°C, 5 to 35 kb. American Journal of Science, 276, 1285–1301.

London, D. (1979) Occurrence and Alteration of White Picacho Pegmatites, Arizona. M. S. Thesis, Arizona State University, Tempe, Arizona.

Morimoto, N. and Tokonami, M. (1969) Domain structure of pigeonite and clnoenstatite. American Mineralogist, 54, 725–740.

Nakajima, Y. and Ribbe, P. H. (1980) Alteration of pyroxenes from Hokkaido, Japan, to amphibole, clays, and other biopyriboles. Neues Jahrbuch Fur Mineralogie, Mh., 6, 258–268.

O'Hara, M. J. and Yoder, H. S. (1967) Formation and fractionation of basic magmas at high pressures. Scottish Journal of Geology, 3, 67–117.

Papike, J. J., Ross M. and Clark, J. R. (1969) Crystal-chemical characterization of clinoamphiboles based on five new structure refinements. Mineralogical Society of America Special Paper, 2, 117–136.

Ribbe, P. H. and Nakajima, Y. (1980) Texture and structural interpretation of the alteration of pyroxenes to other biopyriboles (abstr.). Transactions American Geophysical Union (EOS), 61, 408.

Robinson, P., Jaffe, H. W., Ross, M. and Klein, C., Jr. (1971) Orientation of exsolution lamellae in clinopyroxenes and clinoamphiboles: consideration of optimal phase boundaries. American Mineralogist, 56, 909–939.

Robinson, P., Ross, M. Nord, G. L., Jr., Smyth, J. R. and Jaffe, H. W. (1977) Exsolution lamellae in augite and pigeonite: fossil indicators of lattice parameters at high temperature and pressure. American Mineralogist, 62, 857–873.

Smith, P. P. K. (1977) An electron microscope study of amphibole lamellae in augite. Contributions to Mineralogy and Petrology, 59, 317–322.

Smyth, J. R. (1977) Peraluminous omphacite: cation vacancies in mantle-derived pyroxene (abstr.). Transactions American Geophysial Union (EOS), 58, 523.

Smyth, J. R. (1980) Cation vacancies and the crystal chemistry of breakdown reactions in kiberlitic omphacites. American Mineralogist, 65, 1185–1191.

Smyth, J. R. and Hatton, C. J. (1977) A coesite-sanidine grospydite drom the Roberts Victor kimberlite. Earth and Planetary Science Letters, 34, 284–288.

Thompson, J. B., Jr. (1970) Geometrical possibilities for amphibole structures: Model biopyriboles (abstr.). American Mineralogist, 55, 292–293.

Thompson, J. B., Jr. (1978) Biopyriboles and polysomatic series. American Mineralogist, 63, 239–249.

Veblen, D. R. and Burnham, C. W. (1978a) New biopyriboles from Chester, Vermont: I. Descriptive mineralogy. American Mineralogist, 64, 1000–1009.

Veblen, D. R. and Burnham, C. W. (1978b) New biopyriboles from Chester, Vermont: II. The crystal chemistry of jimthompsonite, clinojimthompsonite, and chesterite, and the amphibole-mica reaction. American Mineralogist, 63, 1053–1073.

Veblen, D. R. and Buseck, P. R. (1977) Petrologic implications of hydrous biopyriboles intergrown with igneous pyroxene (abstr.). Transactions American Geophysical Union (EOS), 58, 1242.

Veblen, D. R. and Buseck, P. R. (1979a) Chain-width order and disorder in biopyriboles. American Mineralogist, 64, 687–700.

Veblen, D. R. and Buseck, P. R. (1979b) Serpentine minerals: intergrowths and new combination structures. Science, 206, 1398–1400.

Veblen, D. R. and Buseck, P. R. (1979c) Replacement rules for hydration reactions in biopyriboles (abstr.). Geological Society of America Abstracts with Programs, 11, 532.

Veblen, D. R., Buseck, P. R. and Burnham, C. W. (1977) Asbestiform chain silicates: New minerals and structural groups. Science, 198, 359–365.

Wood, B. J. and Henderson, C. M. B. (1978) Composition and unit cell parameters of synthetic non-stoichiometric tschermakitic clinopyroxenes. American Mineralogist, 63, 66–72.

Yada, K. (1967) Study of chrysotile asbestos by a high resolution electron microscope. Acta Crystallographica, 23, 704–707.

Yada, K. (1979) Microstructures of chrysotile and antigorite by high resolution electron microscopy. Canadian Mineralogist, 17, 679–691.

Yamaguchi, Y., Akai, J. and Tomita, K. (1978) Clinoamphibole lamellae in diopside of garnet lherzolite from Alpe Arami, Bellinzona, Switzerland. Contributions to Mineralogy and Petrology, 66, 263–270.

Manuscript received, February 18, 1981;
accepted for publication, July 23, 1981.